

**Interim report on the technical
support for global validation of
ERS Wind and Wave Products
at ECMWF**

(Project Ref. 15988/02/I-LG)

Saleh Abdalla and Hans Hersbach

Research Department

May 2003

*This paper has not been published and should be regarded as an Internal Report from ECMWF.
Permission to quote from it should be obtained from the ECMWF.*



For additional copies please contact

The Library
ECMWF
Shinfield Park
Reading
RG2 9AX
library@ecmwf.int

Series: ECMWF Technical Memoranda

A full list of ECMWF Publications can be found on our web site under:

<http://www.ecmwf.int/publications/>

©Copyright 2003

European Centre for Medium Range Weather Forecasts
Shinfield Park, Reading, RG2 9AX, England

Literary and scientific copyrights belong to ECMWF and are reserved in all countries. This publication is not to be reprinted or translated in whole or in part without the written permission of the Director. Appropriate non-commercial use will normally be granted under the condition that reference is made to ECMWF.

The information within this publication is given in good faith and considered to be true, but ECMWF accepts no liability for error, omission and for loss or damage arising from its use.



Abstract

Contracted by ESRIN, ECMWF is involved in the global validation and monitoring of geophysical products from the ERS-2 satellite. The parameters under consideration are the fast delivery (FD) surface wind speed and significant wave height products from the Radar Altimeter instrument (URA product), wave products from the Synthetic Aperture Radar instrument (UWA product) and surface wind speed and direction from the Scatterometer (UWI product). Validation is performed against corresponding parameters from the ECMWF atmospheric and wave model data as well as in-situ wave buoys, whenever possible.

The project (15988/02/I-LG), which runs from 1 April 2002 to 31 March 2004, is the continuation of previous contracts with ESTEC. This note is an interim report on the activities performed within the scope of this contract. Besides, an overview of the performance of the URA, UWA and UWI products obtained from standardized monitoring tools, a description of dedicated scientific research is included. The considered period are the last five years with special attention to the beginning of 2002 until April 2003. For this latter period, the attitude control of the ERS-2 platform was performed in zero-gyro mode (ZGM), which was installed after an on-board failure in January 2001. It led to degradations of data quality of all three products.

The degradation of altimeter and SAR wave data due to ZGM piloting was acceptable. Data received from these instruments seems to be stable and of good quality, especially since March 2002. In general, apart from the overestimation of small wave heights, altimeter wave heights are rather stable and of good quality. A quadruple collocation (ERS altimeter, buoy, model hindcast and model analysis) exercise over the whole years of 2000 and 2001 suggests a relative error in altimeter wave heights of about 7%. This was further confirmed by a quintuple collocation (ENVISAT RA-2 Ku-band, ERS altimeter, buoy, model first guess and model analysis) exercise between July 2002 and March 2003. Altimeter wind speeds suffered from serious degradations during several intervals since early 2000. Apart from those intervals the wind product is rather acceptable.

The SAR wave height data passed through several phases of performance. Although, degradation at one stage in the past can be attributed to an incorrect calibration factor in the inversion software used at ECMWF, others may be related, but not with a strong support, to the ERS stability due to the loss of the gyroscopes.

The on-board failure had a decremental effect on the quality of the scatterometer wind product. Global dissemination was suspended. In December 2001 ESRIN started to provide UWI data to a selected group, for the purpose of quality assessment only. A close monitoring at ECMWF showed a steady improvement of its quality, with a jump at the introduction of a new orbit control system, ESACA, in February 2003. The monitoring revealed several shortcomings, and indicated that presently, the potential quality of the data is higher than before the failure in January 2001. In parallel, work on CMOD5, a new geophysical model function (GMF) relating wind speed and direction to scatterometer backscatter, was completed. It has a higher internal consistency than CMOD4, which is the GMF currently used by ESA, and is able to produce more realistic wind vectors, especially for strong winds.

1 Introduction

The ERS mission is a great opportunity for the meteorological and ocean-wave community. The wind and wave products from ERS-1/2 provide an invaluable data set with global coverage. They provide some kind of benchmarks against which model products can be validated. In addition, they are assimilated in the models to improve the nowcast. On the other hand, consistent model products, especially first-guess products, can be used to validate and monitor the performance of the satellite products.

The European Centre for Medium-Range Weather Forecasts (ECMWF) has been supporting the European Space Agency (ESA) since the beginning of the ERS-1 mission in performing the global validation and long-term performance monitoring of the wind and wave products. These products are retrieved from three instruments, defining three Fast Delivery (FD) products that are received at ECMWF in BUFR format. Significant wave height and surface wind speed (URA product) are obtained from the Radar altimeter (RA). Ocean-wave

spectra (UWA product) are from the Synthetic Aperture Radar (SAR). Surface wind speed and direction (UWI product), finally, are retrieved from the Active Microwave Instrument (AMI) scatterometer. In-house developed monitoring tools are used for a comparison of these products with corresponding parameters from the ECMWF atmospheric and wave model. Whenever possible, these tools include a comparison with in-situ wave buoys. In addition, tests are performed on the internal consistency of the underlying observed quantities measured by the three instruments.

This support has been carried out within the framework of several contracts with ESA. The current contract (15988/02/I-LG), which is supervised by the European Space Research Institute (ESRIN), runs from 1 April 2002 to 30 March 2004. Findings from the monitoring activities described above are summarized in monthly or cyclic (depending on the product) data quality and validation reports. Besides of giving an overview on instrument performance and scientific interpretation, these reports include recommendations to ESA for refinements of calibrations, further algorithm development and model tuning. Such recommendations are based on a long-term analysis of the relevant parameters.

In addition to these monitoring activities, dedicated studies on data quality and related scientific research has been carried out. These embrace, among others, collocation studies, algorithm development and the incorporation of ERS wind and wave data in the ECMWF assimilation system. As a result, altimeter wave heights have been assimilated in the ECMWF wave model since 15 August 1993 (Janssen *et al.* 1997). Scatterometer winds were introduced in the atmospheric variational assimilation system on 30 January 1996 (for a description of its impact, see Isaksen and Janssen 2003). The assimilation of SAR wave spectra in the ECMWF wave model, finally, was realized from 13 January 2003 onwards.

This memorandum is an interim report of the present contract. It gives an overview of the performance of the Wind and Wave products over a period of about five years, with specific attention to the year 2002 and the first part of 2003. During this latter period, the ERS-2 Attitude and Orbit Control System (AOCS) operated in zero-gyro mode (ZGM). It was introduced in June 2001, and replaced the Extra Back-up Mode (EBM) in which ERS-2 had been operating since an on-board failure on 17 January 2001. Since that event, none of the six gyroscopes has been available for the platform's attitude control. It had a negative, though acceptable, effect on the quality of the altimeter and SAR data. However, it had a decremental effect on retrieved scatterometer winds, since these are very sensitive to the large errors in the yaw angle positioning. It resulted in the suspension of dissemination of scatterometer data.

In Section 2, the long-term performance of altimeter data will be considered on the basis of time-series of their mean values and histograms. In addition, work on a collocation study (quadruple and quintuple) that allowed for the estimation of the error in the significant wave height product, will be described. A similar exercise could be carried out later for other products. An overview of the long-term performance of the SAR significant wave height will be presented in Section 3.

Although scatterometer data had become unusable, a feasibility study at ESRIN had learned that there was a potential for restoring the original data quality. With the purpose for independent quality assessment, ESRIN has provided UWI data to a selective group from 12 December 2001 onwards. At ECMWF, the quality of this data has been assessed and monitored since. Results will be described in Section 4. In addition to this monitoring task, research on the development of a new geophysical model function (GMF) was performed. A GMF relates the surface wind vector to the scatterometer backscatter signal. In the near future, the resulting GMF, named CMOD5, is to replace CMOD4, the GMF on which the C-band scatterometer winds has been based for a number of years. Starting point was a prototype that was developed at KNMI (Haan, de and Stoffelen, 2001), where, due to a lack of resources, its completion was inhibited. Its derivation and impact on the wind product will be described in Section 4, as well.

In Section 5, conclusions and recommendations are presented. The report ends with three appendices. Ap-

pendix A and B give rather detailed descriptions of the processing of URA and UWA data respectively, as performed at ECMWF. In Appendix C, finally, a list of relevant changes to the ECMWF ocean-wave and atmospheric model is given.

Acronyms

AMI	Active Microwave Instrument
AN	ECMWF ANalysis
AOCS	Attitude and Orbit Control System
ASCAT	Advanced SCATterometer
BUFR	Binary Universal Form for the Representation of meteorological data
CMOD	C-band Geophysical MODEL function
DES	Digital Earth Sensor
DNMI	(Det) Norwegian Meteorological Institute
EBM	Extra Back-up Mode
ECMWF	European Centre for Medium-range Weather Forecasts
ENVISAT	ENVIronmental SATellite
ESA	European Space Agency
ERS	European Remote sensing Satellite
ESACA	Ers Scatterometer Attitude Corrected Algorithm
ESTEC	European Space research and TEchnology Centre
ESRIN	European Space Research INstitute
EUMETSAT	EUropean organization for the exploration of METeorological SATellites
FD	Fast Delivery product
FG	ECMWF First Guess
FGAT	First Guess at Appropriate Time
GMF	scatterometer Geophysical Model Function
GTS	Global Telecommunication System
IFS	Integrated Forecast System
KNMI	Koninklijk Nederlands Meteorologisch Instituut
MPI	Max-Planck-Institut for meteorology, Hamburg
QC	Quality Control
RA	Radar Altimeter
RMSE	Root-Mean Square Error
SAR	Synthetic Aperture Radar
SI	Scatter Index
SWH	Significant Wave Height
URA	User FD Radar Altimeter product
UWA	User FD SAR WAve product
UWI	User FD scatterometer WInd product
WAM	third-generation ocean-WAve Model
ZGM	Zero-Gyro Mode

2 The altimeter URA product

2.1 Quality Control

The received RA observations pass through a quality control (QC) procedure to remove all erroneous and suspicious records. Specifically, the QC process can be divided into two levels: a basic level (which ensures that each individual observation is within the logical range and is collected over water, during the correct time window) and a secondary level (which ensures that observations passing the basic level within any given sequence of neighboring observations are consistent with each other). It is important to mention that this classification is just for clarification purposes and has no consequence on the quality control process itself. Each sequence of observations consists of 30 individual neighboring observations. Erroneous and suspicious individual observations are removed and the remaining data in each sequence are averaged to form a representative super-observation, providing that the sequence has enough number of "good" individual observations (at least 20 of them). The super-observations are then collocated with the model and the buoy data for the validation purposes. The whole process is outlined in Appendix A.

2.2 Monitoring of the Altimeter Significant Wave Height

In general, RA wave heights are rather stable and of good quality, apart from the overestimation of small wave heights. A histogram of the RA significant wave heights after quality control over the period 21 March to 31 December 2002 is displayed in Figure 1. This period was selected for this long-term plot, as ERS-2 wind and wave products seem to be of the best quality since the ERS-2 Attitude and Orbit Control System (AOCS) started to operate in the Zero Gyro Mode (ZGM) around the beginning of June 2001 (and even before when it was operated in the Extra Back-up Mode, EBM). Apparently, this can be attributed to the yaw control system that makes use of some of the data coming from SAR imagerie processing. This yaw control system was implemented on 4 March 2002 but the impact of this change on the data quality was only evident after the recovery of data dissemination started on 21 March. The time series of the daily global mean of RA wave height after QC over the whole year of 2002 is plotted in Figure 2. It is clear that there is no detectable difference in the behavior of the daily mean wave heights before and after the introduction of the yaw control system on the wave height product.

One point of some concern is the secondary local peak at about 2.5 m in the ERS-2 RA wave height distribution shown in Figure 1. The same peak appears in all monthly histograms since December 1996 (and possibly before). Pierre Queffelec (personal communications, 2003) pointed out that such a peak does not exist in the histograms of the corresponding off-line product (OPR1). A possible explanation of this peak is the existence of two wave-height populations can be ruled out since a similar peak does not appear in the corresponding WAM histograms (refer to the monthly reports). It is worthwhile mentioning that a similar peak does not occur in the corresponding ENVISAT RA-2 histograms for both Ku and S-bands. Figure 3 shows a monthly RA-2 Ku-band histogram for the month of March 2003. Another possible explanation is that this peak is due to the inability of the ERS-2 altimeter in sensing wave heights below 60 cm, can be ruled out as well. ENVISAT S-band altimeter has the same inability but its histogram does not have a similar secondary peak.

The time series of the global bias between RA significant wave height super-observations and the WAM wave heights over more than 5 years (from 11 September 1997 to 7 April 2003) is plotted in Figure 4. Both 5-day and 30-day running means of the bias are plotted. A similar plot for the root mean square differences (RMSE) is shown in Figure 5, in the same order. It should be noted that the erroneous RA observations collected after the recovery from the ERS-2 anomaly in January-February 2001 (when the platform left with a single gyro) were filtered out in Figures 4 and 5. The general trend of obtaining better agreement between the altimeter

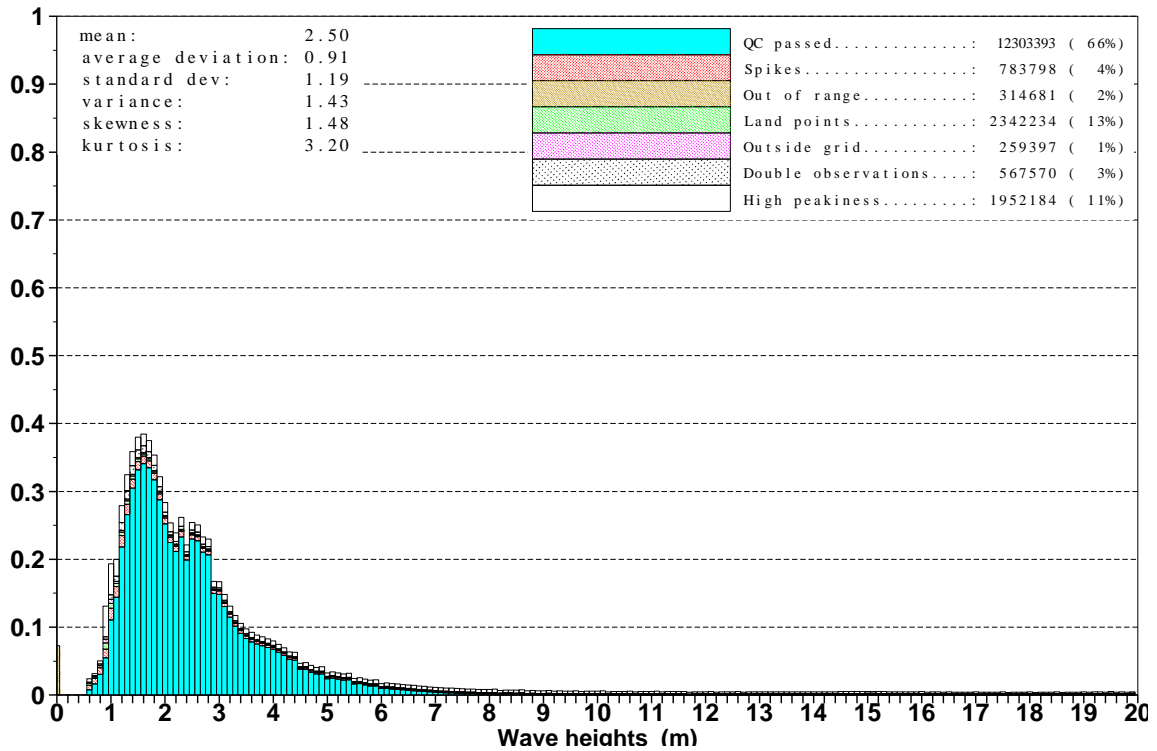


Figure 1: Distribution of ERS-2 RA significant wave heights after QC during the period from 21 March to 31 December 2002.

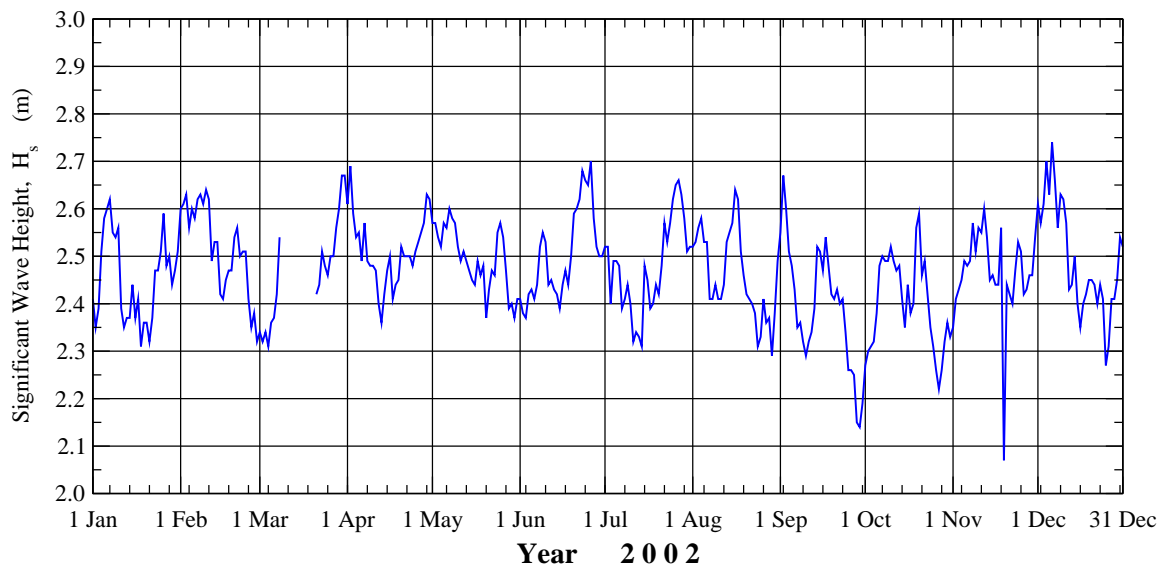


Figure 2: Daily global mean of ERS-2 RA significant wave height after QC during the whole year of 2002.

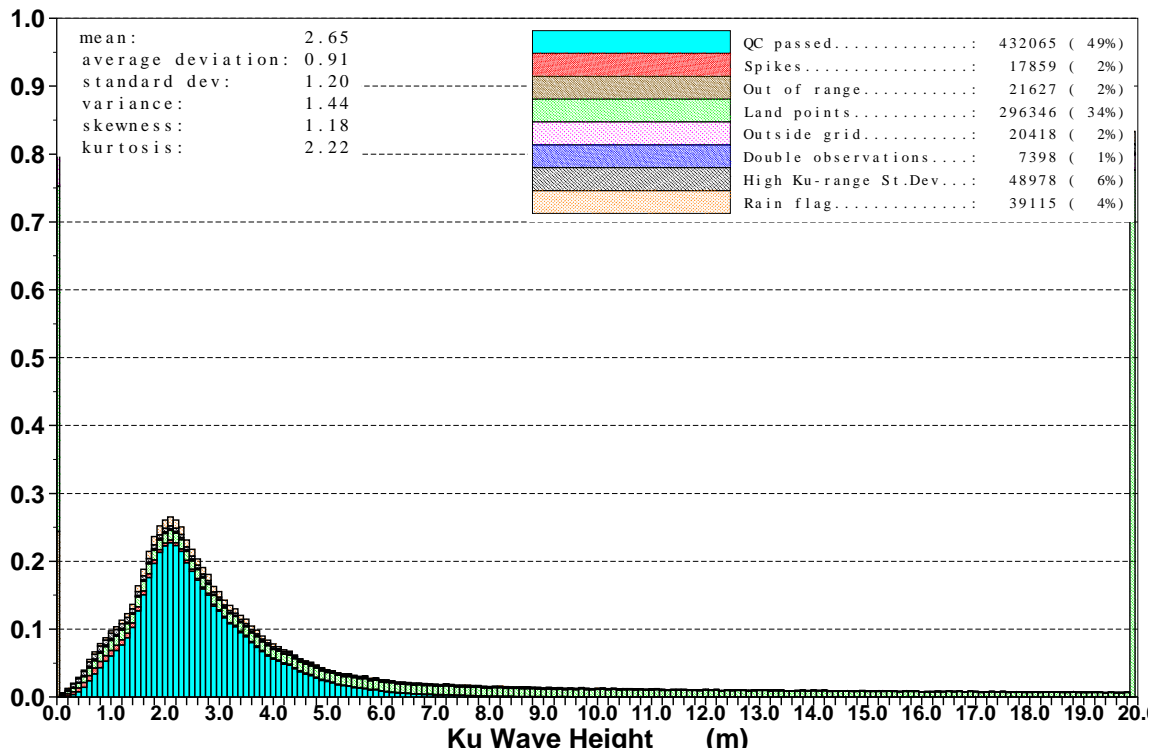


Figure 3: Distribution of ENVISAT RA-2 Ku-band significant wave heights after QC for the whole month of March 2003.

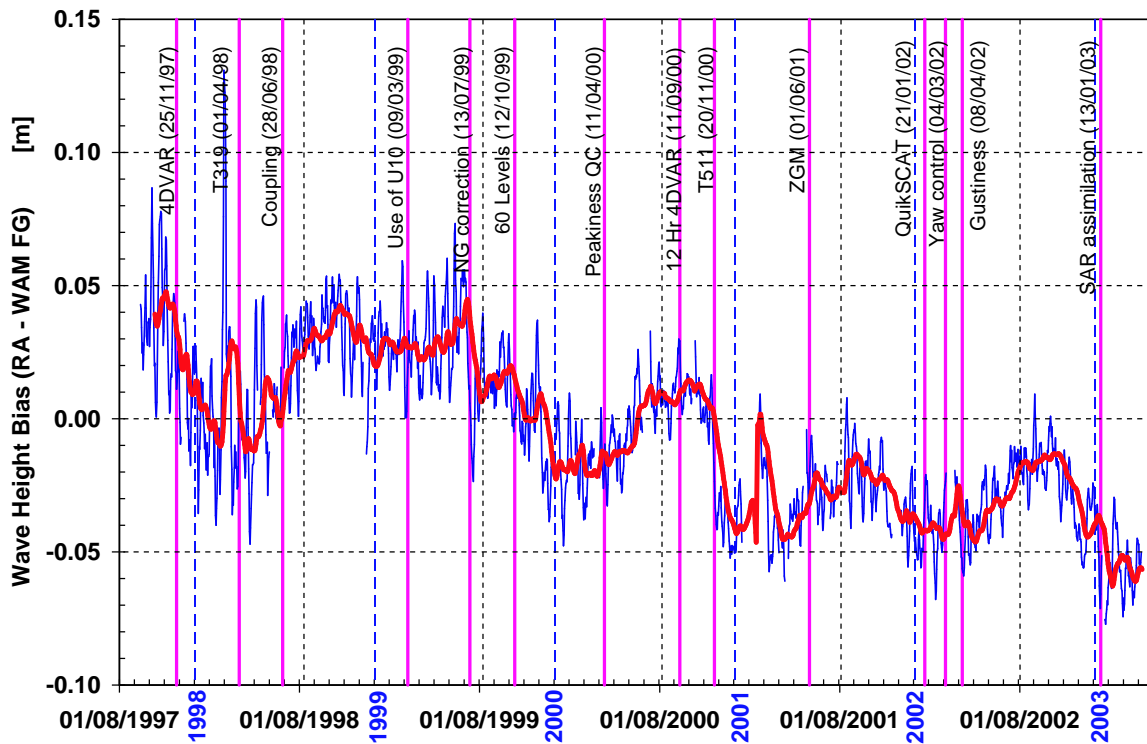


Figure 4: Global bias between ERS-2 RA significant wave height super-observations and WAM model during the period from 11 September 1997 to 7 April 2003. (Thin navy line is 5-day running mean, while thick red line is 30-day running mean.)

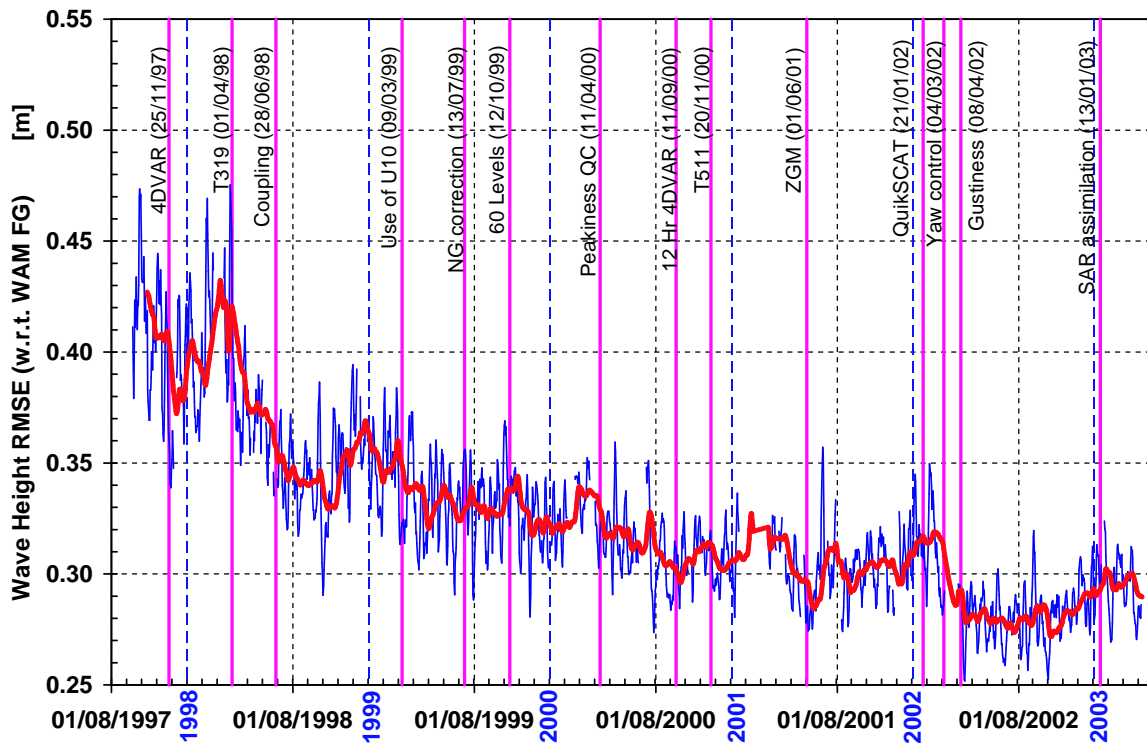


Figure 5: Global RMSE between ERS-2 RA significant wave height super-observations and WAM model during the period from 11 September 1997 to 7 April 2003. (Thin navy line is 5-day running mean, while thick red line is 30-day running mean.)

and WAM over the years is clear. Several model changes can be associated with significant changes in the bias and/or the RMSE values. For example, the introduction of the altimeter wave height correction based on the non-gaussianity of the sea surface elevation (on 13 July 1999) and the introduction of the new atmospheric model resolution TL511 (on 20 November 2000) led to significant reduction in bias (i.e. increase in WAM wave heights). One can also recognize the worsening of the agreement (increase of RMSE) after June 2001 when the ZGM was activated on the platform AOCs. Apparently the introduction of yaw control system on 4 March 2001 (together with a model change about a month later) has a considerable impact towards reducing the RMSE. Furthermore, several model changes, especially the introduction of the IFS horizontal resolution T319 and the coupling between WAM and IFS, had significant impact towards the reduction of the RMSE.

A direct comparison between the observations produced from two instruments provides information only regarding about the "accuracy" of each instrument with respect to the other. This means that it is not possible to estimate the "absolute accuracy" of each instrument. However, it is possible to show that under certain conditions the "absolute accuracy" of each instrument can be estimated provided there are enough instruments (at least 3) measuring the same truth roughly at the same time and at the same location [refer to Janssen et al. (2003) for the details]. Observation from each measuring system is assumed to be a linear function of the truth and an error. Along this line, all the quadruple collocations of ERS-2 altimeter, buoy, model hindcast and model analysis over two full years (2000-2001) were collected and analyzed. To minimize the contribution of the dislocation, both in space and time, to the error estimates, the collocated quintuplets are rejected if the difference between the model estimates at the location of the RA observation and the buoy location exceeds 5%. Furthermore, the fast delivery ERS-2 significant wave heights suffer from a systematic error at low wave heights, as it is not able to detect any wave height below 60 cm. Therefore, we only considered collocations with wave heights in excess of 1 m. The resulted number of "trusted" collocations used in the error estimates

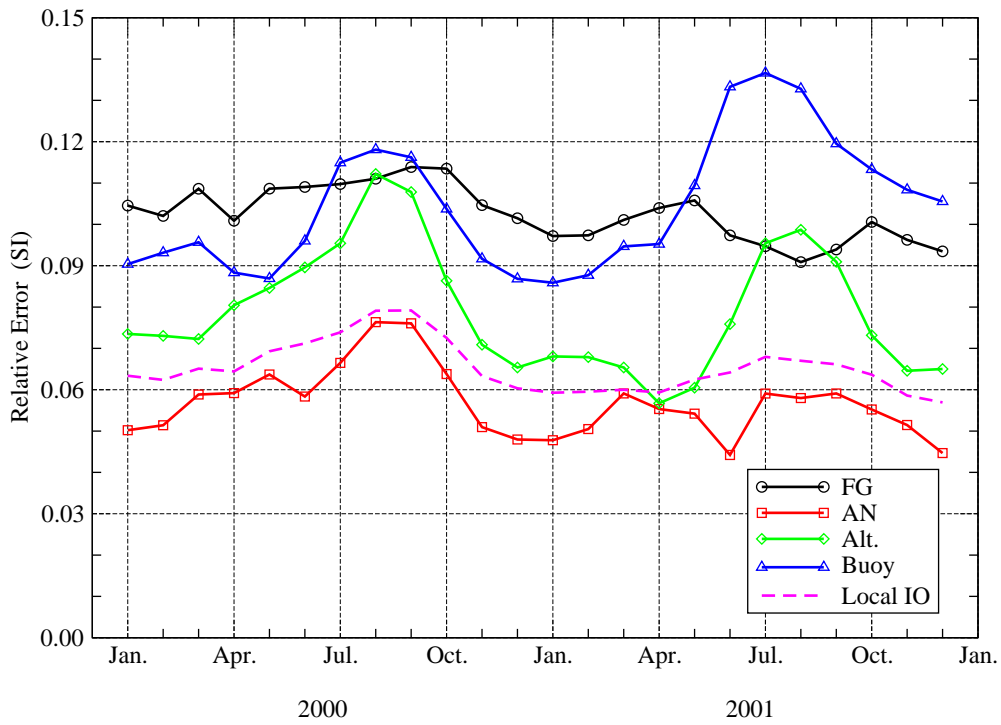


Figure 6: Monthly relative error of first-guess (FG), analyzed (AN), ERS-2 RA (Alt) and buoy wave height. (Maximum collocation difference is 5%, wave heights greater than 1 m.)

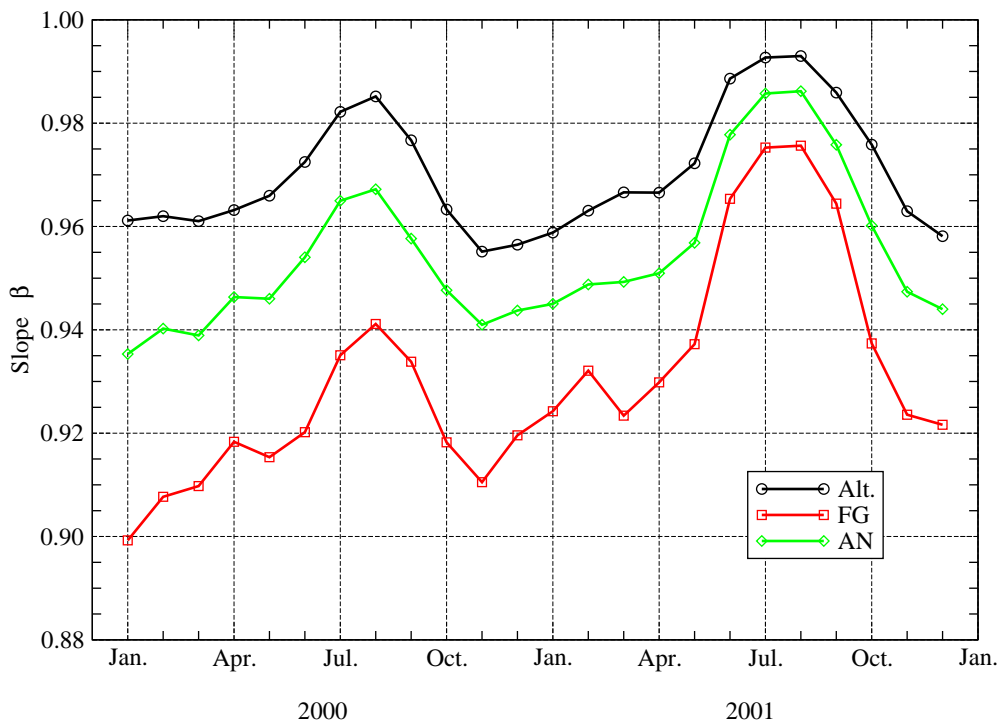


Figure 7: Monthly slopes with respect to buoy waves for ERS-2 RA (Alt), first-guess (FG) and analyzed (AN) wave height. (Maximum collocation difference is 5%, wave heights greater than 1 m.)

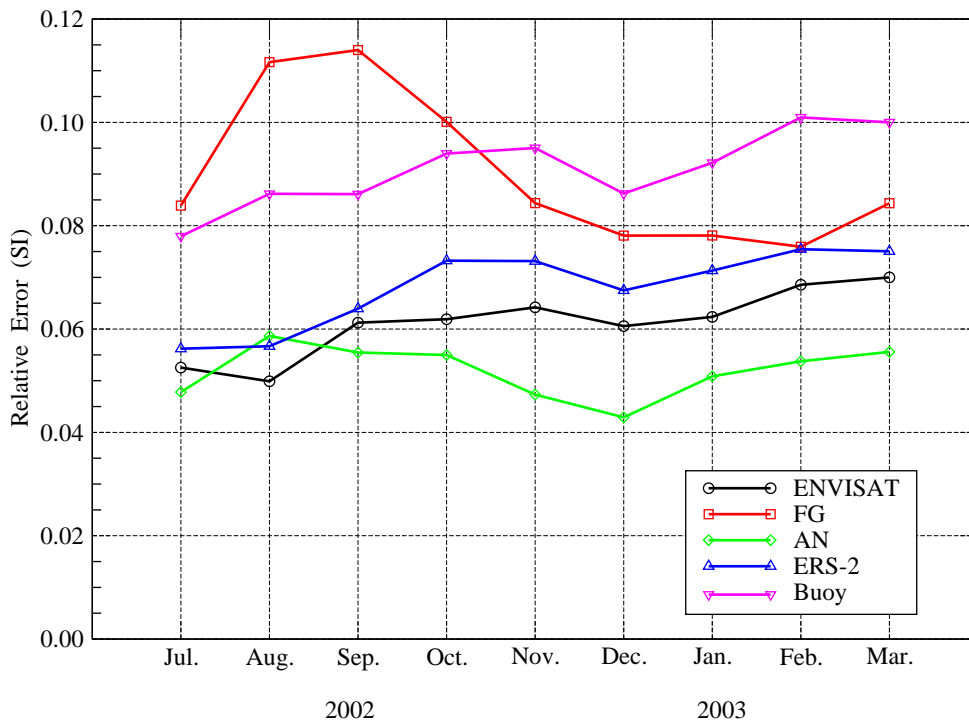


Figure 8: Monthly relative error of ENVISAT RA-2, first-guess (FG), analyzed (AN), ERS-2 RA and buoy wave height during the period from 18 July 2002 to 14 March 2003. (Maximum collocation difference is 5%, wave heights greater than 1 m.)

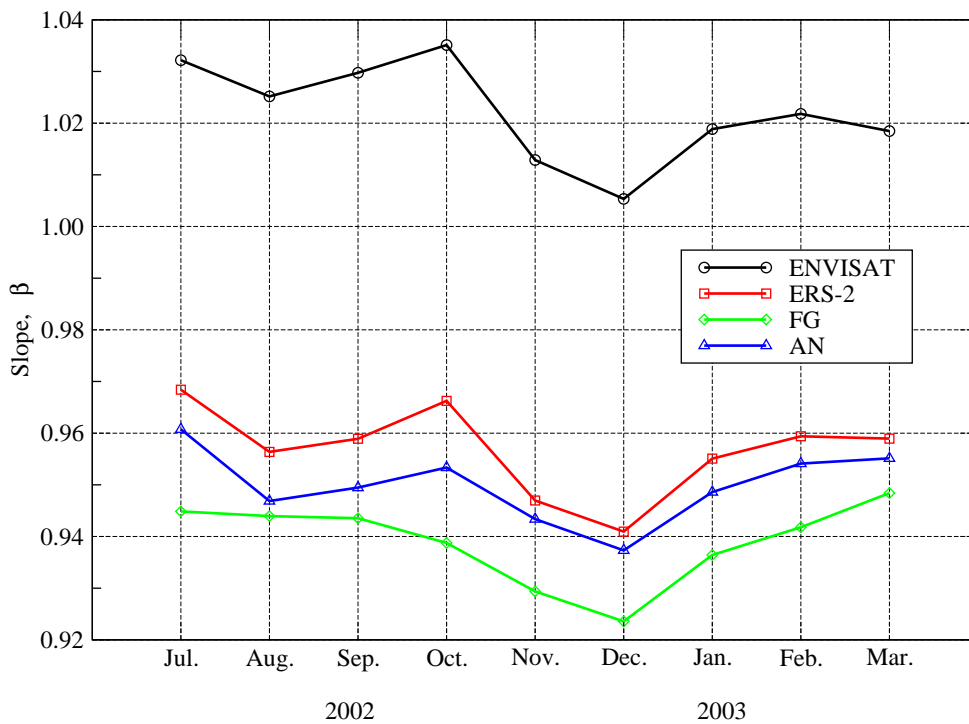


Figure 9: Monthly slope with respect to buoy waves of ENVISAT RA-2 Ku-band, ERS-2 RA, first-guess (FG) and analyzed (AN) wave height during the period from 18 July 2002 to 14 March 2003. (Maximum collocation difference is 5%, wave heights greater than 1 m.)

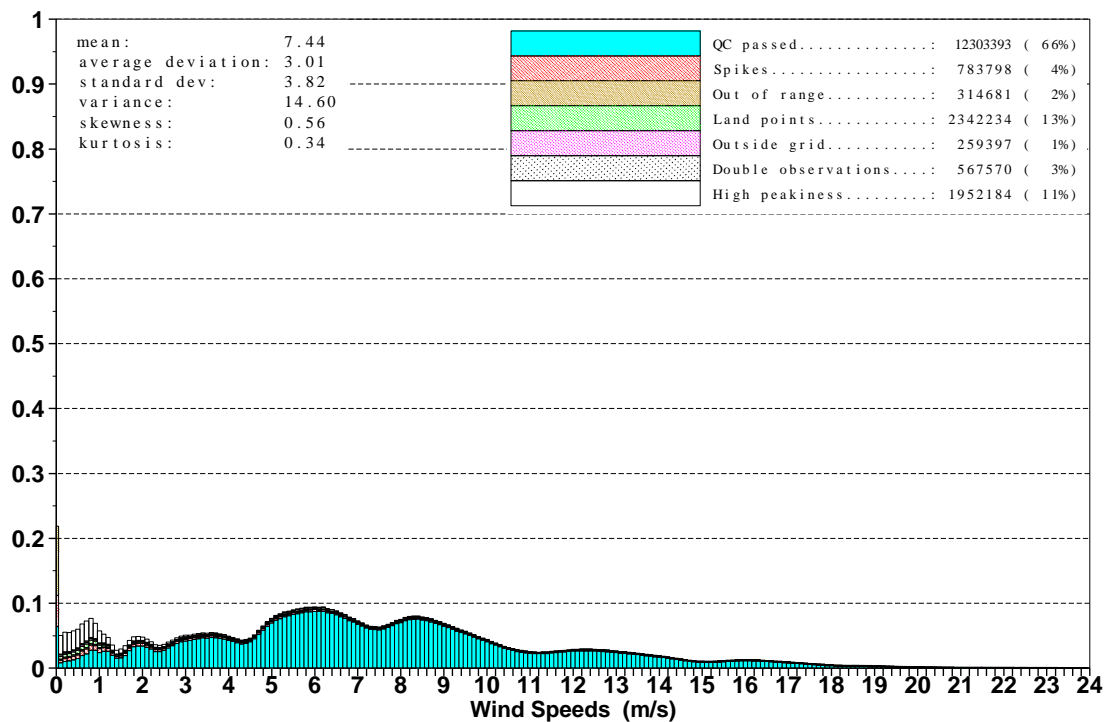


Figure 10: Distribution of ERS-2 RA wind speeds after QC during the period from 21 March to 31 December 2002.

is around 8000. The results of this exercise over the whole years of 2000 and 2001 suggest that the relative random error in ERS-2 altimeter wave height super-observations is about 6.5%. Furthermore, Janssen et al. (2003) estimate the relative error in the altimeter individual observations to be around 10%. The monthly relative error of the different measurement systems including the altimeter can be seen in Figure 6. If the buoy observations are selected as the reference for the comparison, ERS-2 wave heights are too low by 3% with the monthly distribution shown in Figure 7. These findings were further confirmed by a quintuple collocation of ENVISAT RA-2 Ku-band, ERS altimeter, buoy, model first guess and model analysis exercise for the period between July 2002 and March 2003. The results are plotted in Figures 8 and 9 (Janssen and Abdalla, 2003). Another important outcome of the work of Janssen et al. (2003) is that it would be more appropriate to average over 15 individual observations in order to obtain the ERS-2 super-observations. This would slightly increase the relative error of the ERS-2 altimeter wave height super-observation (slightly above 7%).

2.3 Monitoring of the Altimeter Surface Wind Speed

In general, RA wind speed observations are not as good as the wave heights. They suffer several periods of degraded quality especially after the loss of the gyros. The "sun blinding effect" is responsible for most of the degradation. Sun blinding occurs due to a special configuration of the Earth, the satellite, and the Sun in which the Digital Earth Sensor (DES, which is the active sensor used to determine the platform attitude) looks directly in the sun. This occurs around latitude 40° S for the ascending tracks only and for a period going from mid-January to early March each year. This impact on the data started since the change from the three-gyro to the single-gyro piloting in early 2000. The situation became worse after the activation of the ZGM on the AOCs since June 2001. Fortunately, wind speed product started to be of rather good quality after the implementation of the new yaw control system in March 2002 (apart from the sun blinding period).

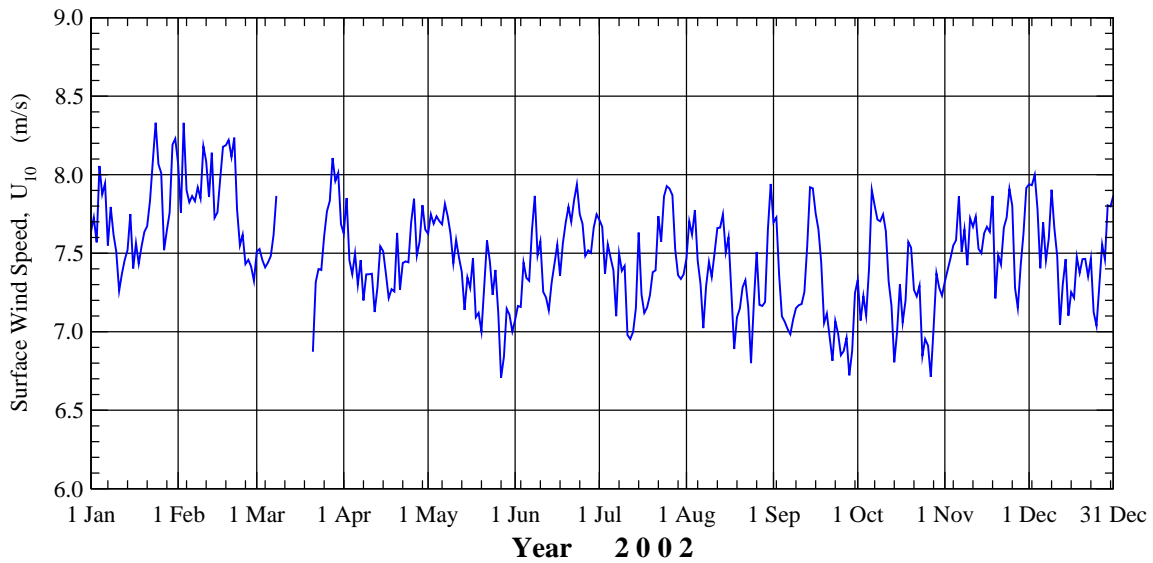


Figure 11: Daily global mean of ERS-2 RA wind speed after QC during the whole year of 2002.

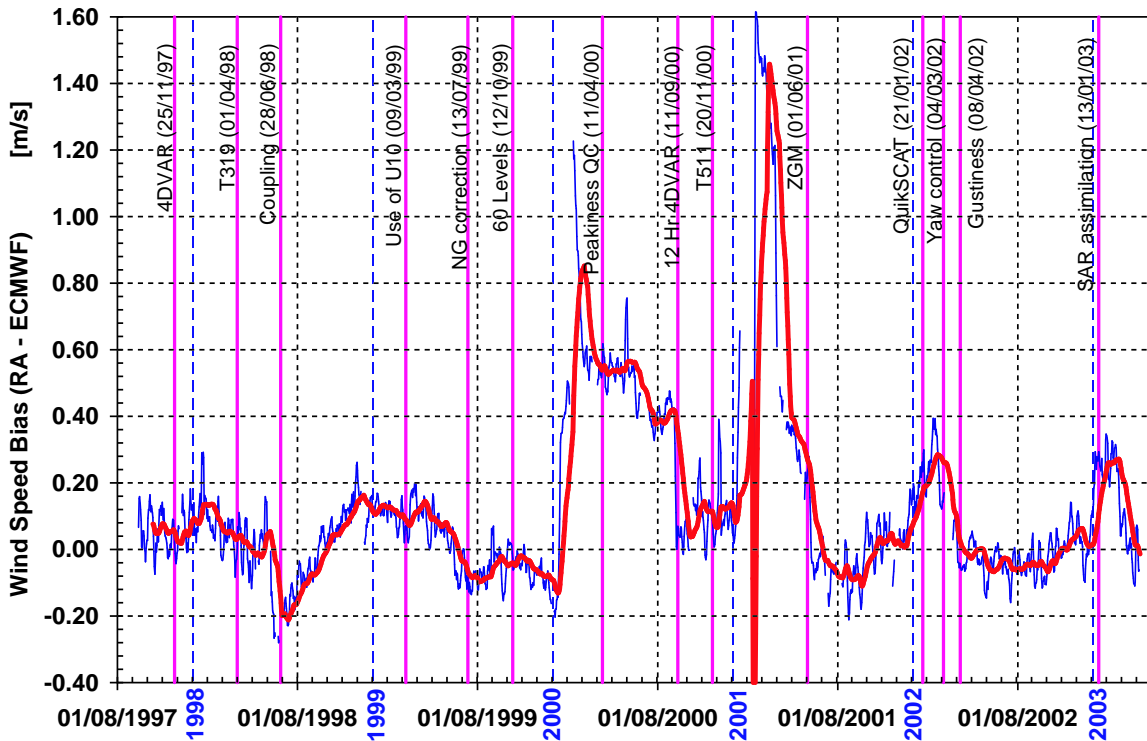


Figure 12: Global bias between ERS-2 RA wind speed super-observations and ECMWF model during the period from 11 September 1997 to 7 April 2003. (Thin navy line is 5-day running mean, while thick red line is 30-day running mean.)

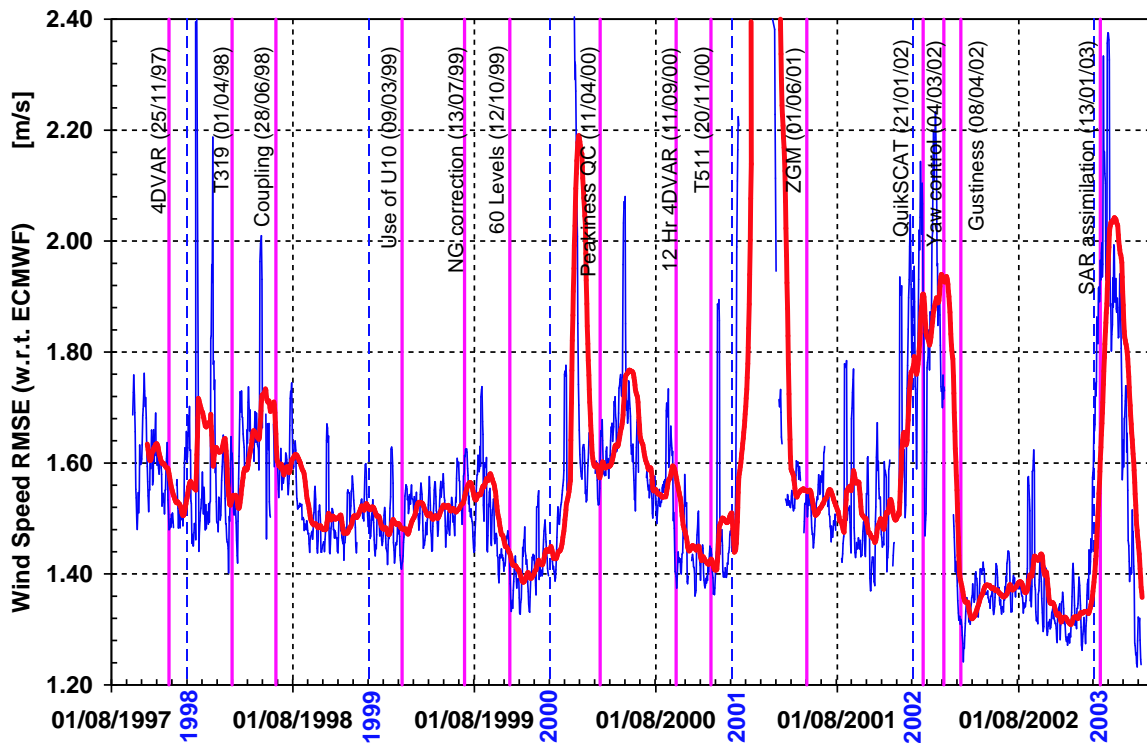


Figure 13: Global RMSE between ERS-2 RA wind speed super-observations and ECMWF model during the period from 11 September 1997 to 7 April 2003. (Thin navy line is 5-day running mean, while thick red line is 30-day running mean.)

A histogram of the RA wind speeds after quality control over the period 21 March to 31 December 2002 is displayed in Figure 10. The time series of the daily global mean of RA wave height after QC over the whole year of 2002 is plotted in Figure 11. The rather high wind speeds during the sun blinding period from mid-January to early March is rather clear.

The time series of the global bias between RA wind speed super-observations and the ECMWF model wind speeds over more than 5 years (from 11 September 1997 to 7 April 2003) is plotted in Figure 12. Both 5-day and 30-day running means of the bias are plotted. A similar plot for the root mean square differences (RMSE) is shown in Figure 13. Unlike the similar wave plots the erroneous RA observations collected after the recovery from the ERS-2 anomaly in January-February 2001 were filtered out. One can also recognize the worsening of the agreement (increase of RMSE) after June 2001 when the ZGM was activated on the platform AOCs. Compared to ECMWF winds, the best performance of the RA winds happened after the implementation of the new yaw control system in March 2002 as can be clearly seen in Figures 12 and 13. Unlike the wave height comparison, it is difficult to distinguish the impact of the model changes on the statistics. This is mainly due to the instability of the RA wind product.

2.4 Monitoring of the Altimeter Backscatter

RA backscatter is the raw observation that is converted to wind speed. Logically it is the parameter that suffers the actual degradation during the last few years. As there is no means to access an independent source of data to compare those measurements against, we retain to the self-consistency tests.

A histogram of the RA backscatter after quality control over the period 21 March to 31 December 2002 is displayed in Figure 14. The time series of the daily global mean of RA wave height after QC over the whole

year of 2002 is plotted in Figure 15. The rather low backscatter values during the sun-blinding period from mid-January to early March are evident.

To display the longer-term variation of the backscatter mean values, Figure 16 shows the monthly mean backscatter values since December 1996. One can recognize two different patterns: before and after January 2000. The sun-blinding effect is clearly seen by the relatively lower mean values. Clearly, there were peak monthly mean values on July each year. Those peaks do not exist anymore since the year 2000. Furthermore, the backscatter monthly histograms have some differences. Figure 17 shows a typical histogram before January 2000 with a well-defined single peak. The secondary peaks are very small. On the other hand, a typical recent histogram looks similar to Figure 14. A secondary peak is emerging and sometimes it becomes as important as the main peak. The reason after such change in behavior is not clear.

3 The Synthetic Aperture Radar UWA product

3.1 Quality control

For the UWA product, each SAR record is examined to ensure that all parameters are within the acceptable range. Records that pass this basic QC are collocated with the corresponding WAM spectra. The WAM spectra serve as a first-guess to the SAR inversion procedure. The observed SAR spectra are then inverted to calculate the corresponding wave spectra by an iterative method based on the forward closed integral transformation (what is termed as the MPI scheme). Further QC is applied based on the outcome of the inversion process. The whole process is outlined in Appendix B.

3.2 Monitoring of the Synthetic Aperture Radar wave height

A long-term monitoring of the significant wave height computed from the inverted ERS-2 SAR spectra was performed. It is worthwhile mentioning that there was a bug in the SAR inversion software introduced in June 1998. The software was unable to properly handle the SAR data with the new calibration procedure introduced around that time. This bug was fixed in the WAM model change on 20 November 2000. Furthermore, SAR data are assimilated in the wave model since 13 January 2003.

The time series of the global bias between SAR significant wave heights and the WAM model wave heights over a period of about 5 years (from 28 June 1998 to 7 April 2003) is plotted in Figure 18. Both 5-day and 30-day running means of the bias are plotted. A similar plot for the RMSE is shown in Figure 19. During the period before the introduction of the bug fix, one can notice the consistent and slowly improving agreement between the model and the SAR wave heights. Apart from its impact on the RMSE, the bug caused SAR wave heights to be overestimated as compared to the model as can be seen in Figure 18. During that period, two noticeable bias drops occurred at the times when the RA wave height correction due to the non-gaussianity effects and when the RA quality control based on the peakiness factor were introduced. The SAR inversion bug fix together with the IFS resolution change to T511 (horizontal resolution of 40 km) and the increased WAM spectral resolution (30 frequency x 24 direction bins) caused a sharp reduction in bias towards negligible values. The impact is very clear in the RMSE plots as well (Figure 19). This situation did not last long due to the loss of the platform gyros early 2001. SAR waves started to be lower with high RMSE. Roughly speaking, SAR wave data were highly degraded during the whole year of 2001. Slight improvement coincides roughly with the implementation of the ZGM in early June 2001. The quality started to be much better since December 2001. The reason for this improvement is unknown. The implementation of the new yaw control system on 4 March 2002 does not seem to have much impact on the SAR wave heights.

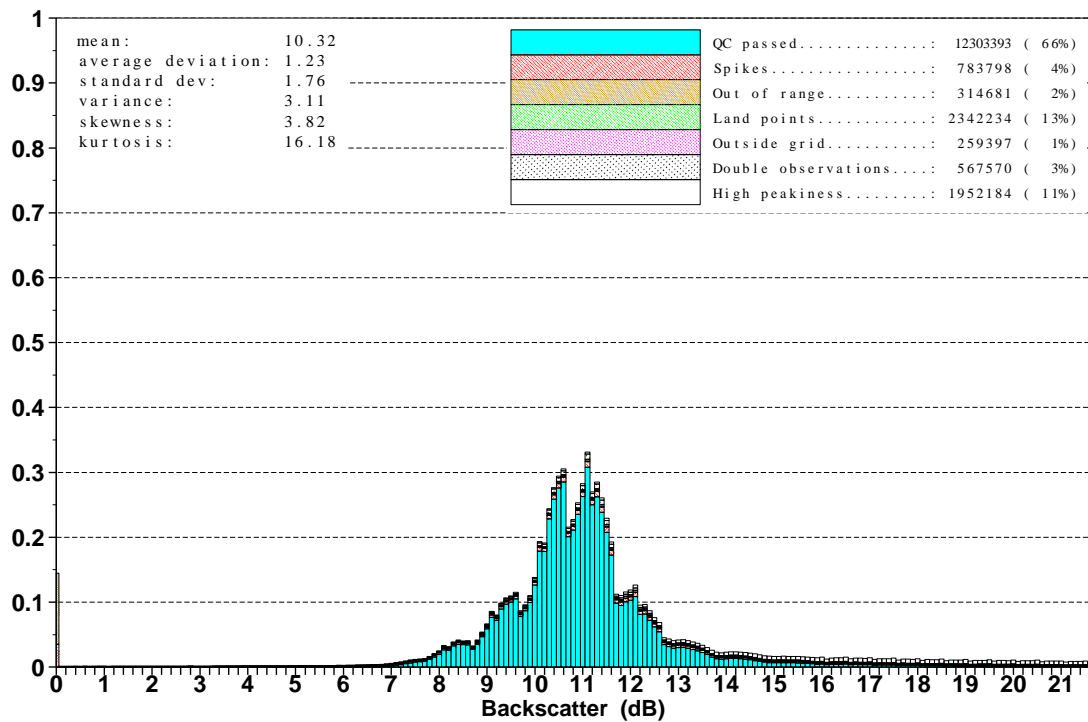


Figure 14: Distribution of ERS-2 RA backscatter coefficients after QC during the period from 21 March to 31 December 2002.

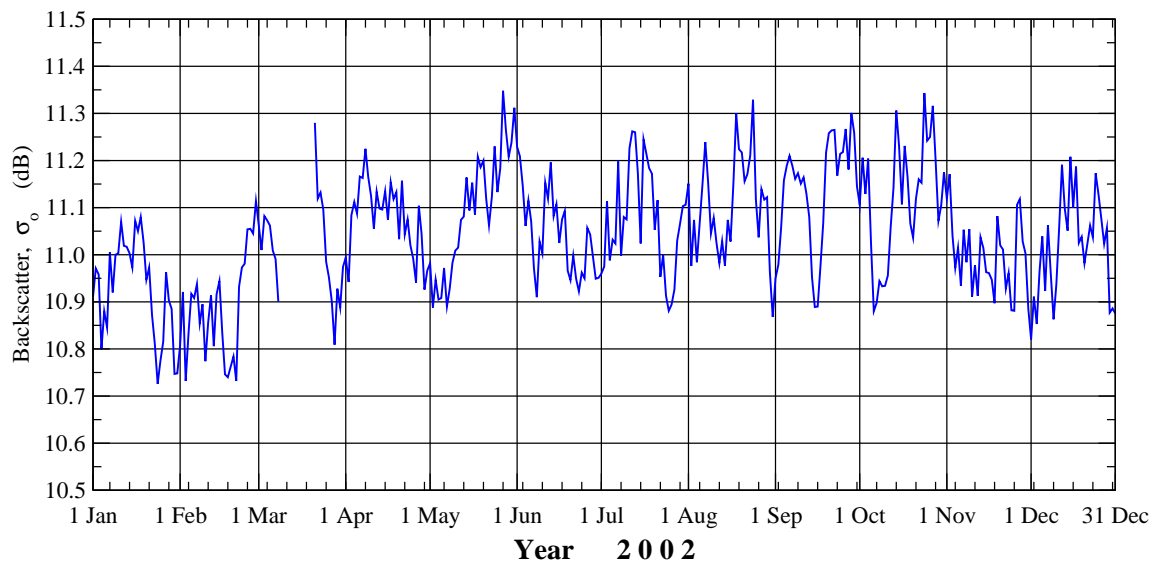


Figure 15: Daily global mean of ERS-2 RA backscatter coefficient after QC during the whole year of 2002.

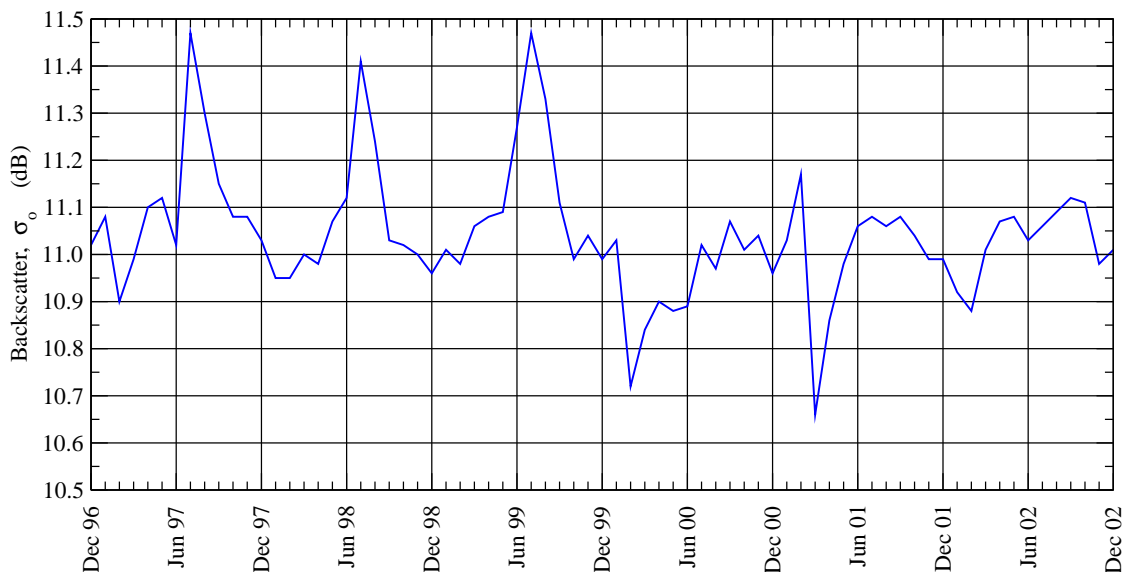


Figure 16: Monthly global mean of ERS-2 RA backscatter coefficient after QC during the period from December 1996 to December 2002.

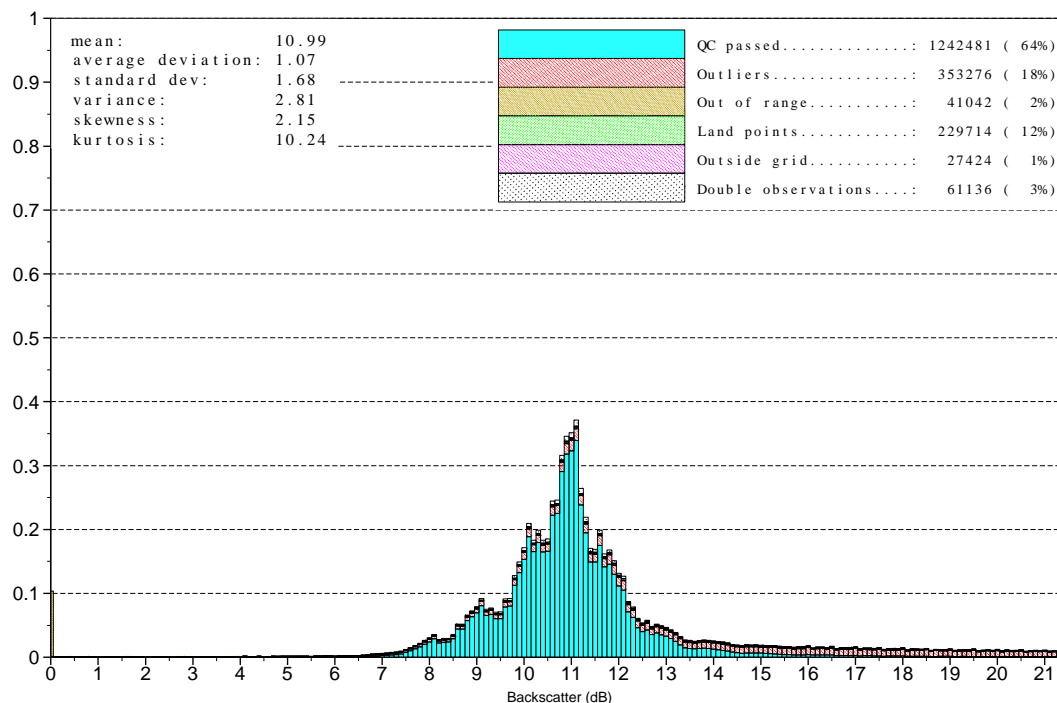


Figure 17: A typical monthly histogram of ERS-2 RA backscatter after QC before January 2000 (this specific example is for October 1999).

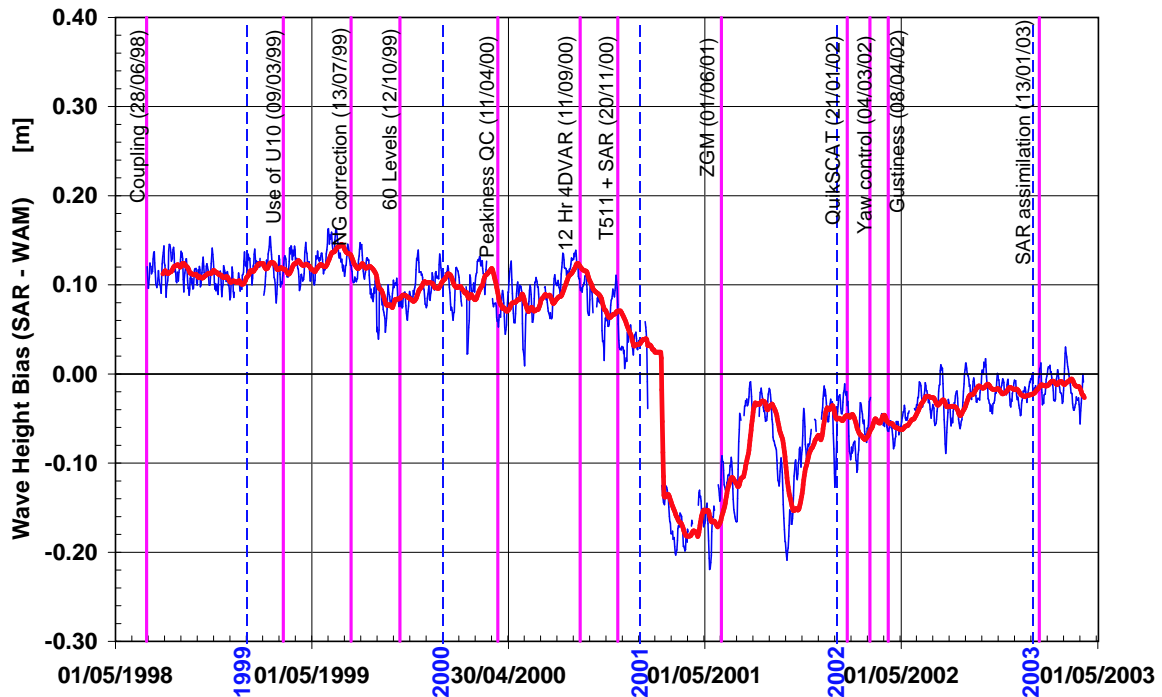


Figure 18: Global bias between ERS-2 SAR significant wave heights and WAM model during the period from 27 June 1998 to 7 April 2003. (Thin navy line is 5-day running mean, while thick red line is 30-day running mean.)

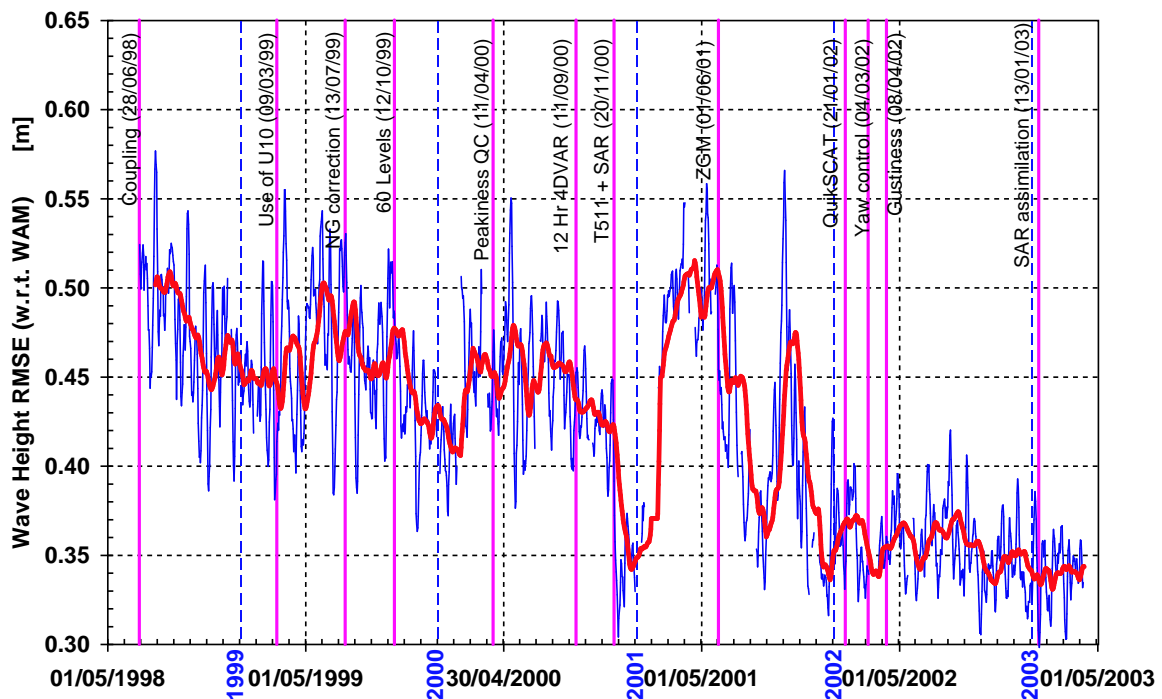


Figure 19: Global RMSE between ERS-2 SAR significant wave heights and WAM model during the period from 27 June 1998 to 7 April 2003. (Thin navy line is 5-day running mean, while thick red line is 30-day running mean.)

4 The Scatterometer UWI product

The logical start of the scatterometer related work performed during the present contract took place at the 20th ASCAT Science Advisory Group Meeting at EUMETSAT (20-21 November 2001). At that time, due to the failure on-board the ERS-2 platform in January 2001, dissemination of ERS-2 scatterometer data had been suspended for 10 months. During that period research at ESRIN had learned that there was a potential for restoring the original quality of the ERS-2 scatterometer winds. For the purpose of quality assessment only, data was to be re-disseminated to a selective group. It was proposed that ECMWF would take care of the validation and monitoring of the internal consistency of the data and the quality of its meteorological content. This task could be performed on the basis of similar tools utilized during the satellites nominal mode (before January 2001).

In addition, it was proposed that ECMWF would complete the work on CMOD5, a new geophysical model function, that in future, should replace CMOD4, the model function on which the C-band scatterometer winds had been based for a number of years. Starting point would be a prototype of CMOD5 that was developed at KNMI (Haan, de and Stoffelen, 2001), where, due to a lack of resources, its completion was inhibited.

The (restricted) dissemination of the UWI wind product started on 12 December 2001. Since the start of this re-distribution, the data has been collected in the ECMWF archives. Its quality has been assessed and monitored since, and results are summarized in a report at the end of each 5-weekly cycle (starting for cycle 69). Interaction with ESRIN has been extensive.

In the first part of this section the setup of the modified monitoring system at ECMWF will be described. The evolution of the quality of the UWI product will be presented as well.

In parallel to these monitoring activities, the work on CMOD5 has been performed. Its final form (June 2002) embraces a complete revision of the mathematical expressions of CMOD4. Its derivation and impact on the wind product will be described in the second part of this section.

4.1 Monitoring of the UWI product in zero-gyro mode

In this section the monitoring activities at ECMWF regarding the UWI data in ZGM is described. Data was collected and monitored from cycles 69 (first data received on 12 December 2001) onwards. The currently latest cycle (82) ended on 24 March 2003.

First a description of the monitoring tools is given, followed by a short history of changes in the UWI data, including a description of the evolution of its quality.

4.1.1 Tools

As mentioned above, the monitoring of the UWI data in ZGM, was based on similar tools as used during the nominal period (before January 2001). These are (including modifications):

- A comparison of wind data with ECMWF first-guess fields. During the nominal period, for these, FGAT winds were used. Their collocation with ERS-2 winds (spatial and temporal resolution of 40km and 1 hour, respectively) is a standard product of the assimilation system at ECMWF. For the ZGM data this accuracy could not be met, since ERS-2 winds have not been assimilated since January 2001. Instead, first-guess winds with a temporal resolution of 3 hours (spatial resolution is still 40km) are the best

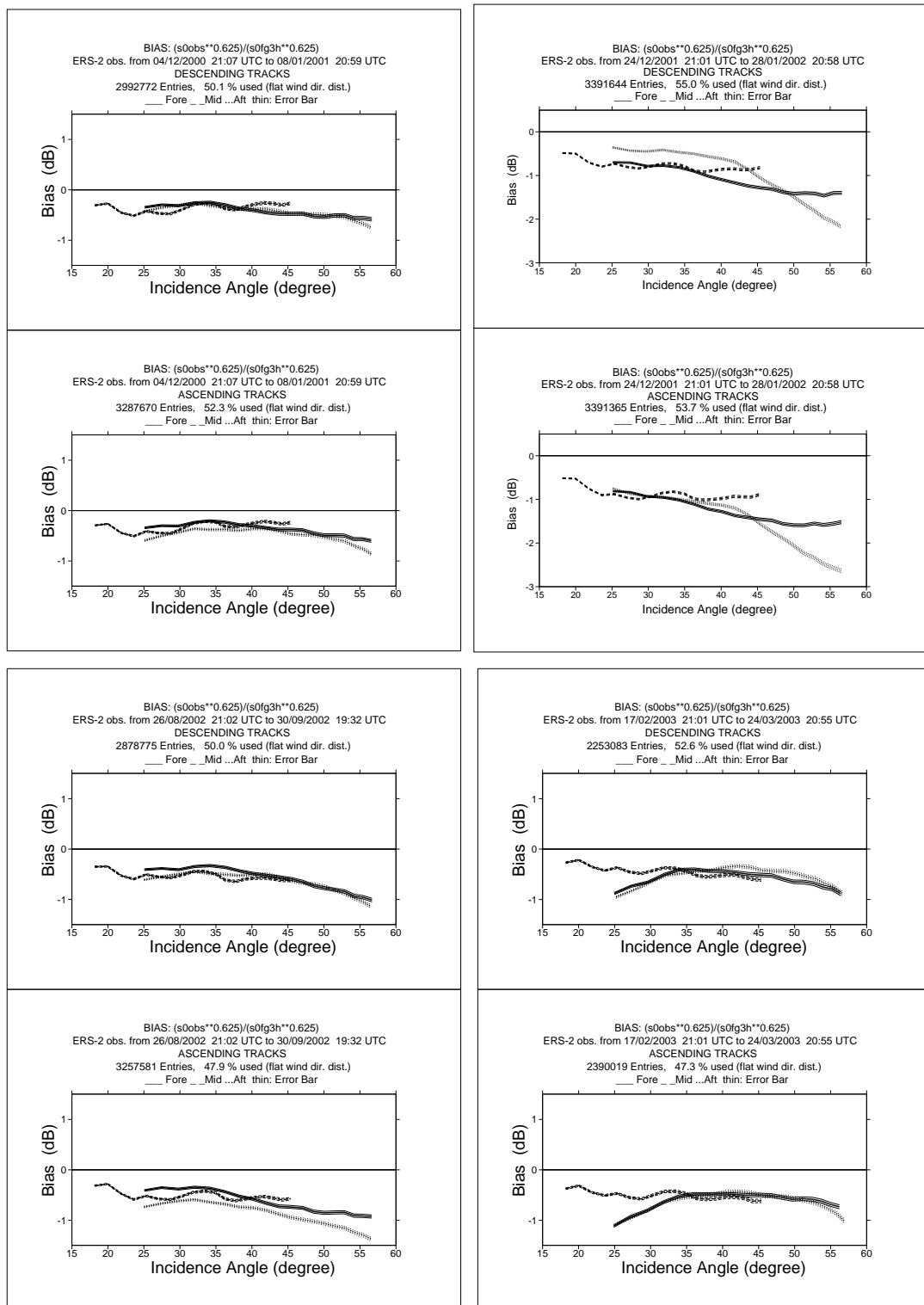


Figure 20: Ratio of $\langle \sigma_0^{0.625} \rangle / \langle \text{CMOD4}(\text{FGAT})^{0.625} \rangle$ converted in dB for the fore beam (solid line), mid beam (dashed line) and aft beam (dotted line), as a function of incidence angle for descending and ascending tracks of data within cycles 59 (top left), 70 (top right), 77 (bottom left) and 82 (bottom right). The thin lines indicate the error bars on the estimated mean. First-guess winds are based on the in time closest (+3h, +6h, +9h, or +12h) T511 forecast field, and are bilinearly interpolated in space.



available. For this, collocation software was to be put in place. Tests for cycle 60 showed that the impact of this change of the time resolution on the monitoring results is very modest.

- Besides the assessment of the quality of UWI winds, the characteristics of the ERS-2 scatterometer winds as they were assimilated, used to be monitored as well. These winds were, like the UWI winds, based on CMOD4. However, prior to the in-house inversion, bias corrections were applied to the backscatter triplets, and a bias correction was applied to the resulting winds as well. For the ZGM data these assimilated winds were not available. Instead, the proper routines from the assimilation system were merged into the monitoring software. No bias corrections are applied, which allows for a direct comparison between the UWI product (one wind solution only) and the CMOD4 winds (both solutions available). From cycle 74 onwards (14 May 2002), inverted winds on the basis of CMOD5 are monitored as well.
- Normalized distance of backscatter triplets from the two-dimensional cone defined by the geophysical model function. During the nominal period these distances were calculated for the at ECMWF bias-corrected triplets. For the ZGM data these corrections were not performed anymore. As a consequence, new (node-wise) normalization factors were determined, in such a way that it would not affect results during the nominal period.
- Backscatter (σ_0) bias for the three beams (fore, mid, aft) as function of across-node number (1 to 19) and stratified with respect to ascending and descending tracks:

$$dz = \langle z \rangle / \langle z_{\text{CMOD}}(\theta, \text{FGAT}) \rangle,$$

where $z = \sigma^{0.625}$, and θ the node and beam-dependent incidence angle. This bias depends on the underlying model function. Results were and are produced on the basis of CMOD4. Trends in the inter-node and inter-beam relationship indicate changes in the antenna patterns, since trends in the normalizing FGAT winds would appear as integral shifts.

4.1.2 The cyclic reports on the ERS-2 scatterometer

On a 5-weekly basis scatterometer cyclic reports are produced. A PostScript version is transferred to the ESTEC ftp site (ftp.estec.esa.nl) in the directory /home/ftppriv/ecmwf-vr. An ascii version of the text and PostScript versions of the separate figures is sent by e-mail to ESRIN. Notification by e-mail is sent to ESA and ESRIN.

On the basis of the tools described in the previous subsection, the scatterometer cyclic monitoring reports contain the following elements:

- An introduction, giving a general summary of the quality of the UWI data and trends w.r.t. previous cycles. Interruptions in data reception are listed. Also, it is mentioned whether there was an enhancement of solar activity and whether it could have affected the UWI wind product. Finally, it is informed whether the ECMWF assimilation system has changed and whether this had an anticipated impact on the quality of the FGAT winds.
- A section giving a detailed description of performance during the cycle. It includes the following plots.
- Two plots (ascending and descending) of the backscatter biases as described above. Examples (cycle 59, 70, 77 and 82) are given in Figure 20.
- Plots of time series of quantities averaged over 6-hourly data batches and stratified w.r.t. six classes of nodes (1-2, 3-4, 5-7, 8-10, 11-14 and 15-19) of

Monitoring of UWI winds versus First Guess for ERS-2

from 2001121212 to 2003032418

(solid) wind speed bias UWI - First Guess over 6h (deg.)

(dashed) wind speed standard deviation UWI - First Guess over 6h (deg.)

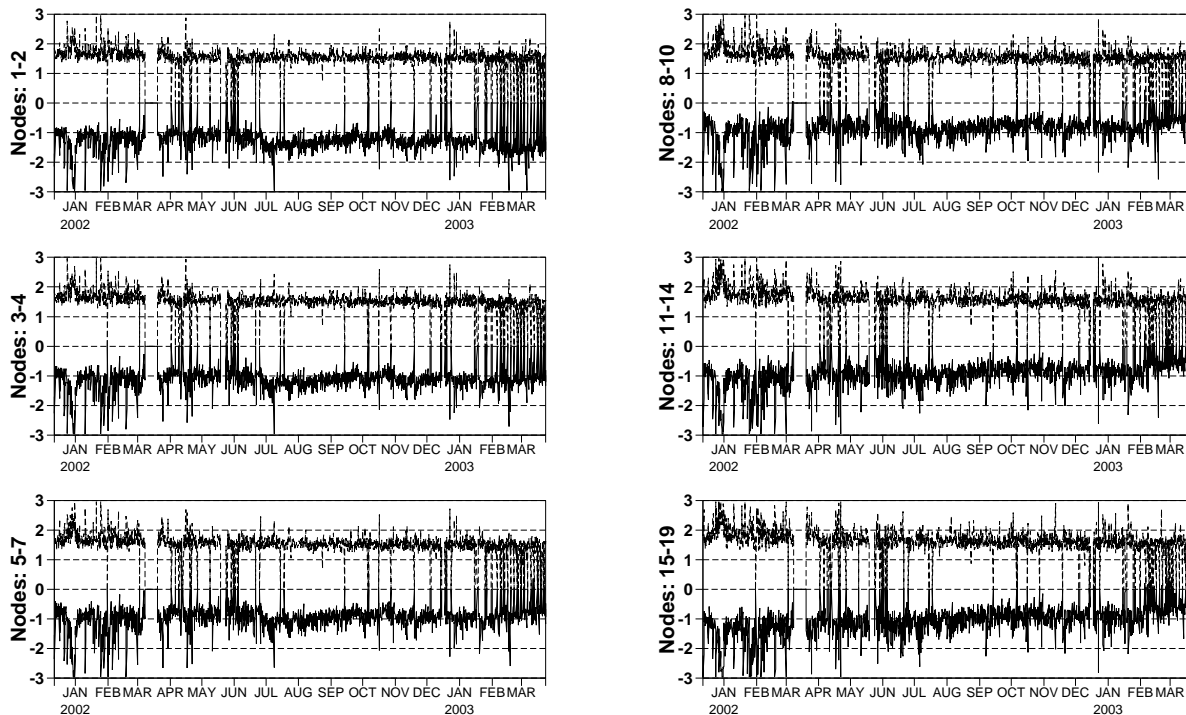


Figure 21: History plot of UWI wind speed versus FGAT

- The normalized distance to the cone, the fraction of rejected data on the basis of CMOD4 inversion or ESA flags, and the total number of received data over sea.
- Bias and standard deviation of UWI versus FGAT for wind speed and direction. An example (but extending over several cycles) is given in Figure 21
- The same for de-aliased CMOD4 winds
- Time series of the (not in time averaged) difference between the fore and aft incidence angle of node 10 (cycle 81 and 82). This asymmetry is induced by errors in yaw attitude control.
- Histograms for the entire cycle (scatter plots) are displayed between UWI and FGAT wind speed and direction. Occasionally scatterplots for CMOD4 and UWI winds are displayed, while plots between CMOD5 and UWI wind speed have been produced from cycle 74 onwards.
- Global plots of locations where UWI winds were more than 8 m/s weaker than FGAT winds. They have been included from cycle 79 onwards. Occasionally UWI and FGAT wind vectors are plotted for specific locations as well.

When important changes in performance occur during a cycle, verification is split up for the different sub-periods.

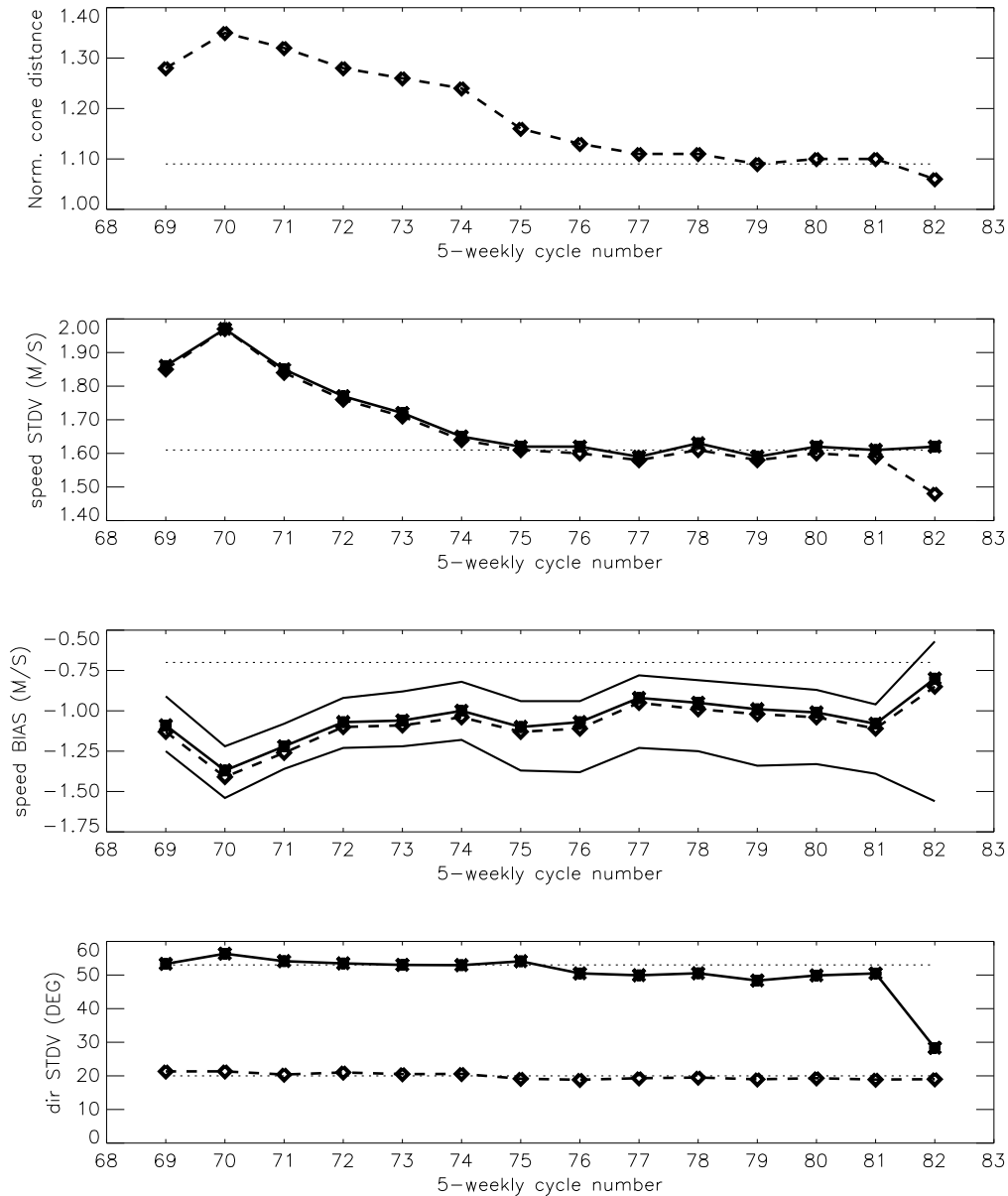


Figure 22: Evolution of the performance of the ERS-2 scatterometer in ZGM averaged over 5-weekly cycles from 12 December 2001 (first data received, cycle 69) to 24 March 2003 (end cycle 82) for the UWI product (solid, star) and de-aliased winds based on CMOD4 (dashed, diamond). Dotted lines represent values for cycle 59 (5 December 2000 to 17 January 2001), i.e. the last stable cycle of the nominal period. From top to bottom panel are shown the normalized distance to the cone (CMOD4 only) the standard deviation of the wind speed compared to FGAT winds, the corresponding bias (for UWI winds the extreme inter-node averages are shown as well), and standard deviation of wind direction compared to FGAT respectively.

4.1.3 Overview of changes in the UWI data and evolution of performance

Before the performance of the UWI data in ZGM (December 2001 onwards) is compared to that of data for the nominal period (before January 2001), one should realize that the following differences in the ECMWF's operational assimilation system (for a complete list see Appendix C) might obscure the results:

- During the nominal period ERS-2 scatterometer data was assimilated. This had a positive effect on the resemblance between UWI winds and FGAT winds, since the latter contain (past) scatterometer information included at earlier assimilation cycles. No ERS-2 scatterometer data was assimilated during the ZGM period.
- On 22 January 2002 the assimilation of QuikSCAT scatterometer data was introduced. Like the case for ERS-2, this will have a positive effect on scatter diagrams between UWI and FGAT winds. Experiments for December 2000, including both ERS-2 and QuikSCAT data indeed showed a noticeable improvement.

Starting from the end of the nominal period, several changes took place. A graphical overview is presented in Figures 21 and 22. They logically defined the following periods:

Before 17 January 2001 (up to cycle 60).

Nominal period. The performance of the UWI product is stable, although in the fall of 2000 there are some problems with the functioning of several of the six on-board gyroscopes. On average, backscatter levels are around 0.5 dB too low (for cycle 59 see top left panel of Figure 20), leading to winds that are on average 0.7 m/s lower than FGAT winds. Although the inter-node and inter-beam sigma biases are small, the UWI wind-speed bias does depend on node number (from -1.1 m/s for low to -0.6 m/s for high incidence angle). It is induced by imperfections in the CMOD4 model function. It does not appear for CMOD5. Standard deviation between UWI and FGAT winds are around 1.6 m/s, and inter-node differences are in the order of 0.05 m/s (for cycle 59 see top left panel of Figure 23). For cycle 59, values of the average cone distance, (UWI - FGAT) and (CMOD4 - FGAT) statistics are displayed by the dotted lines in Figure 22.

17 January 2001 - July 2001 (cycle 60 to 65).

As a result of the on-board failure there are no gyroscopes left for the platform's attitude control. The control system is switched to Extra Back-up Mode. The dissemination of scatterometer data is suspended after 2 February 2001; no cyclic reports could be made for cycles 62 to 68.

July 2001 - 12 December 2001 (cycle 65 to 69).

Introduction of the Zero-Gyro Mode (ZGM). Satellite pointing is achieved through payload data and the digital earth sensor. Although pitch and roll can be controlled accurately, large errors in the yaw attitude (in the order of several degrees) still occur. Such errors especially affect the quality of the scatterometer measurements. Dissemination of scatterometer data remains suspended.

12 December 2001 - 4 February 2003 (cycle 69 to 81).

Restart of dissemination of UWI data, however, to a restricted group of users only. At ECMWF, the monitoring was resumed. Existing tools were updated where necessary (see Section 4.1.2). Besides a number of smaller data gaps, data reception was interrupted from 8 March to 20 March 2002 (cycle 72), from 19 May to 26 May 2002 (cycle 74), and from 15 to 18 December 2002 (cycle 80).

Large errors in yaw, which especially seem to occur around periods of enhanced solar activity, have a large negative impact on the data quality. During these events, part of the backscatter signal is destroyed, which, after inversion, results in far too low winds. Peaks of more than -3 m/s frequently occurred (see Figure 21), especially in January 2002 (cycle 60), which marked a period of considerable solar activity. These incorrect data are also visible in the scatter diagrams of UWI versus FGAT wind speed as anomalously large numbers of

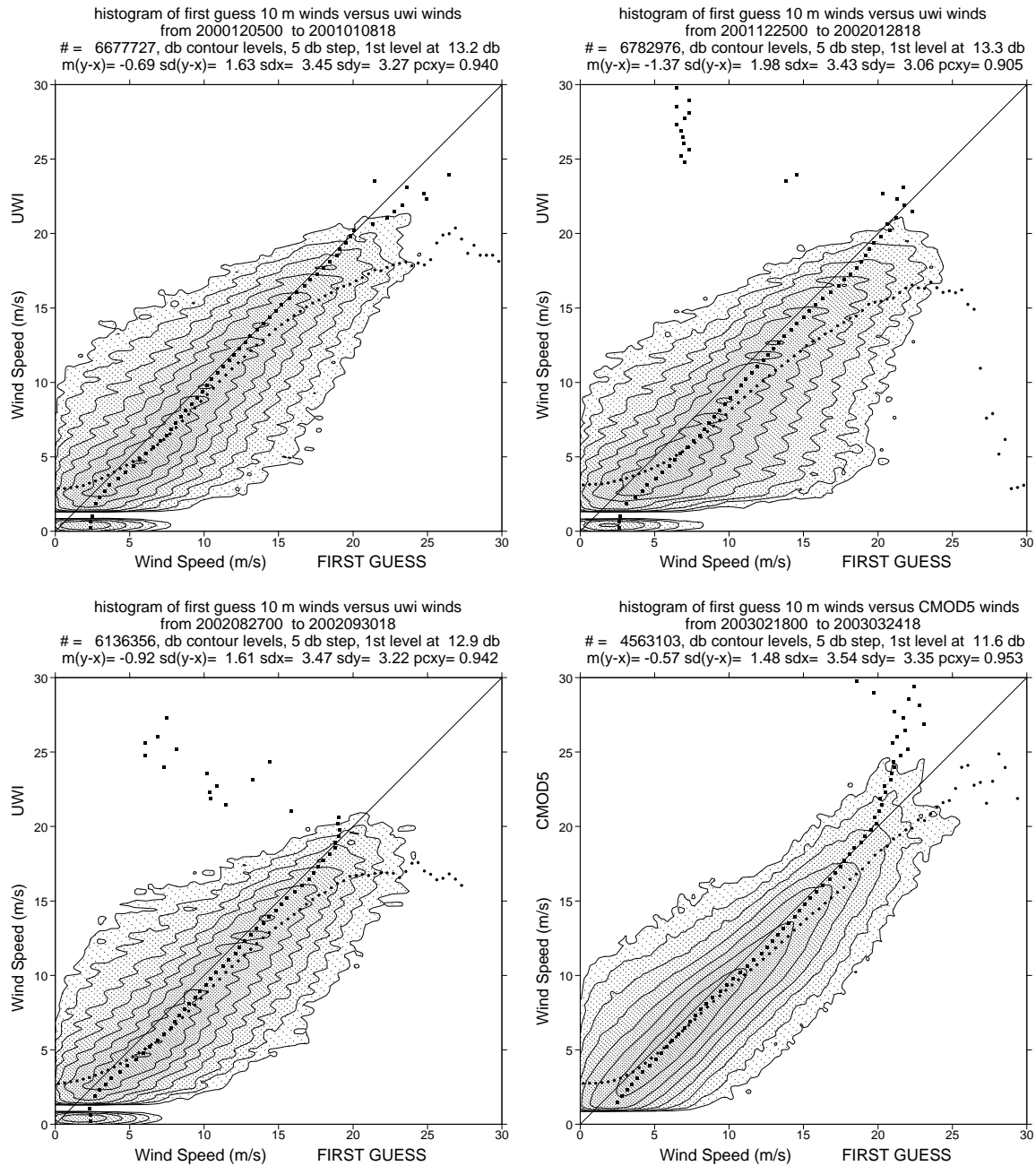


Figure 23: Two-dimensional histogram of FGAT versus UWI wind speeds (top left, cycle 59; top right, cycle 70; bottom left, cycle 77) and of FGAT versus CMOD5 wind speed for cycle 82 (bottom right) for the data kept by the quality control. Circles denote the mean values in the y-direction, and squares those in the x-direction.

collocations between strong FGAT winds and weak UWI winds. For cycle 60 (top right panel of Figure 23), the situation was worst. For later cycles the situation improved (see e.g. lower left panel of Figure 23 for cycle 77). Since cycle 74 no clear signal was found anymore for data that was degraded by solar activity. Although, for cycle 78, a peak in the UWI versus FGAT wind-speed histogram temporarily re-occurred.

Initially extremely large negative biases in the backscatter levels up to -3dB were observed, giving rise to large negative wind-speed biases (i.e., also for data that was less affected by yaw errors). Large inter-node and inter-beam differences (e.g. see top left panel of Figure 20) induced large cone distances. The situation was worst for cycle 60 and slowly improved (see e.g. lower left panel of Figure 20). However, the increasing negative bias towards higher nodes did remain. In line with the average reduction in σ_0 bias, the cone distance and wind-speed biases improved as well (see Figure 22).

For the random error of the UWI and CMOD4 wind speeds a similar trend was observed: worst for cycle 60 (almost 2 m/s) and then first improving rapidly and later stabilizing. From cycle 75 onwards its level has been around the value obtained for the nominal period (see Figure 22). Inter-node differences were usually found to be in the range between 0.1 and 0.15 m/s, i.e., 2-3 times larger than for the nominal period. In general best results are obtained for winds inverted on the basis of CMOD5. Both the negative bias level and standard deviation are smaller for such derived winds.

The performance in wind direction, finally, was affected much less. Although it was initially performing somewhat worse, it has been on the level of the nominal period since cycle 72, and after cycle 75 it has even become better (see Figure 22).

4 February 2003 onwards (cycle 81,...).

Start of the test phase of ESACA, a new processor. This processor is aimed to bring the quality of the UWI product back to its original level. It is capable of adapting on-board filter characteristics appropriately according to an estimation of the yaw attitude error. During the test phase, ESACA data is produced for Kiruna station only. This leads to daily data gaps between approximately 21 UTC and 06 UTC.

The new de-aliasing algorithm (developed at DNMI) appears to work quite well. The UWI winds agree considerably more often to the wind solution that is closest to the FGAT wind direction. Values of standard deviations have dropped from 50 to less than 30 degrees (see Figure 22).

The UWI winds do not coincide anymore with one of the two solutions of (the at ECMWF) inverted CMOD4 winds. CMOD4 winds are of much higher quality than the by ESRIN disseminated UWI winds (see Figure 22). In the meantime, at ESRIN, the cause for this non-ideal situation has been tracked. In begin April 2003 appropriate corrections to ESACA were implemented. UWI winds are now in line with CMOD4 again. The standard deviation w.r.t. FGAT winds is below 1.50 m/s, i.e., about 0.1 m/s better than it used to be during the nominal period.

Large fractions of high k_p values were found, especially for nodes at high incidence angles (more than 50%). Consideration between the UK MetOffice and ESRIN revealed that there is a problem with the BUFR encoding algorithm. A solution is currently being formulated.

In the near range the fore and aft beam show large negative biases in the average backscatter levels. As a result, very large negative wind-speed biases are found for low nodes (-1.6 m/s). At ESRIN, its reason has been identified, and work on an improved antenna pattern is being performed. Besides this asymmetry, the inter-node and inter-beam differences in backscatter levels are small. Their level is comparable to that during the nominal period.

The incidence angles between the fore and aft beam are not equal anymore. They show a rapid variation in time and peaks up to 7 degrees have been observed. This asymmetry reflects errors in the yaw attitude.

Along with improved quality of the CMOD4 winds, the normalized distance to the cone is now below the level of the nominal period. It shows the potentially high quality of the data. Best results are obtained for winds inverted on the basis of CMOD5 (see lower right panel of Figure 23). The standard deviation w.r.t. the FGAT winds is 1.48 m/s; the bias is induced by the negative bias in the backscatter levels.

4.2 CMOD5

4.2.1 Motivation

Since 1993 UWI winds are based on CMOD4. The according to this geophysical model function inverted ERS winds performed during the nominal period within ESA's original instrument specifications. Within these margins, biases of CMOD4 winds are known to exist. For instance, in the low and medium wind-speed range, a wind-speed dependent bias has been observed from a triple collocation study with buoy winds and NCEP model winds (Stoffelen 1998). For the high wind speed sector, CMOD4 is known to over-estimate backscatter, which, after inversion, results into too low winds. Very similar biases are observed when CMOD4 winds are compared to ECMWF FGAT winds (see section 4.1). The wind-speed biases have been present since the start of the monitoring in February 1996. Recent experimental work (Donnelly *et al.* 1999, Carswell *et al.* 1999) confirm the high wind speed trend. They showed that beyond 20 m s^{-1} , the level of backscatter becomes less sensitive to the wind. In fact, for small incidence angles an over-saturation was observed, i.e., for winds larger than 25 m s^{-1} , backscatter starts to decrease. The work of Donnelly *et al.* (1999) and Carswell *et al.* (1999) also indicates that for strong winds both the upwind-downwind asymmetry and the upwind-crosswind term (both defined below) are over-estimated by CMOD4. This over-estimation can also be deduced from an internal consistency check. The distance to the cone appears to rise rapidly towards higher wind speeds, which indicates that the diameter of the CMOD4 cone is inadequate. Although the upwind-downwind and upwind-crosswind terms will not influence the performance of retrieved wind speed too much, they will have an effect on the quality of ambiguity removal, respectively the accuracy of the wind direction.

4.2.2 Method of construction

CMOD5 was determined on the basis of a comparison of ERS-2 scatterometer triplet backscatter measurements with collocated ECMWF FGAT winds. The period between 1 August and 31 December 1998 was considered, for which the ERS-2 satellite was operating in a stable nominal mode. It embraced more than 22,000,000 collocations. For the extreme wind sector (winds larger than 25 m s^{-1}) statistics are sparse, even for a five-months period. In addition, such extreme situations mainly occur for tropical cyclones, for which FGAT winds are known to be on the low side. For this sector, the experimental work of Donnelly *et al.* (1999) and Carswell *et al.* (1999) was used as a guideline. An important ingredient for the determination of CMOD5 was internal consistency. It was demanded that the CMOD5 cone gives a proper representation of the data cone.

Like for most model functions derived for C-band (e.g., the CMOD family) and Ku-band scatterometry (e.g., NSCAT1, QSCAT1), the functional form of CMOD5 is described by:

$$\sigma_0^m(v, \phi, \theta) = B0(v, \theta)(1 + B1(v, \theta) \cos(\phi) + B2(v, \theta) \cos(2\phi))^p,$$

where v and ϕ are the wind speed respectively wind direction relative to the antenna pointing angle, and θ is the incidence angle. $B0$ describes the main dependency on wind speed and incidence angle. The Fourier terms $B1$ and $B2$ define the degree of difference between upwind-downwind respectively upwind-crosswind backscatter measurements. The power $p = 1.6$ for CMOD4 ($p = 1$ for other model functions) was retained in the definition of CMOD5.

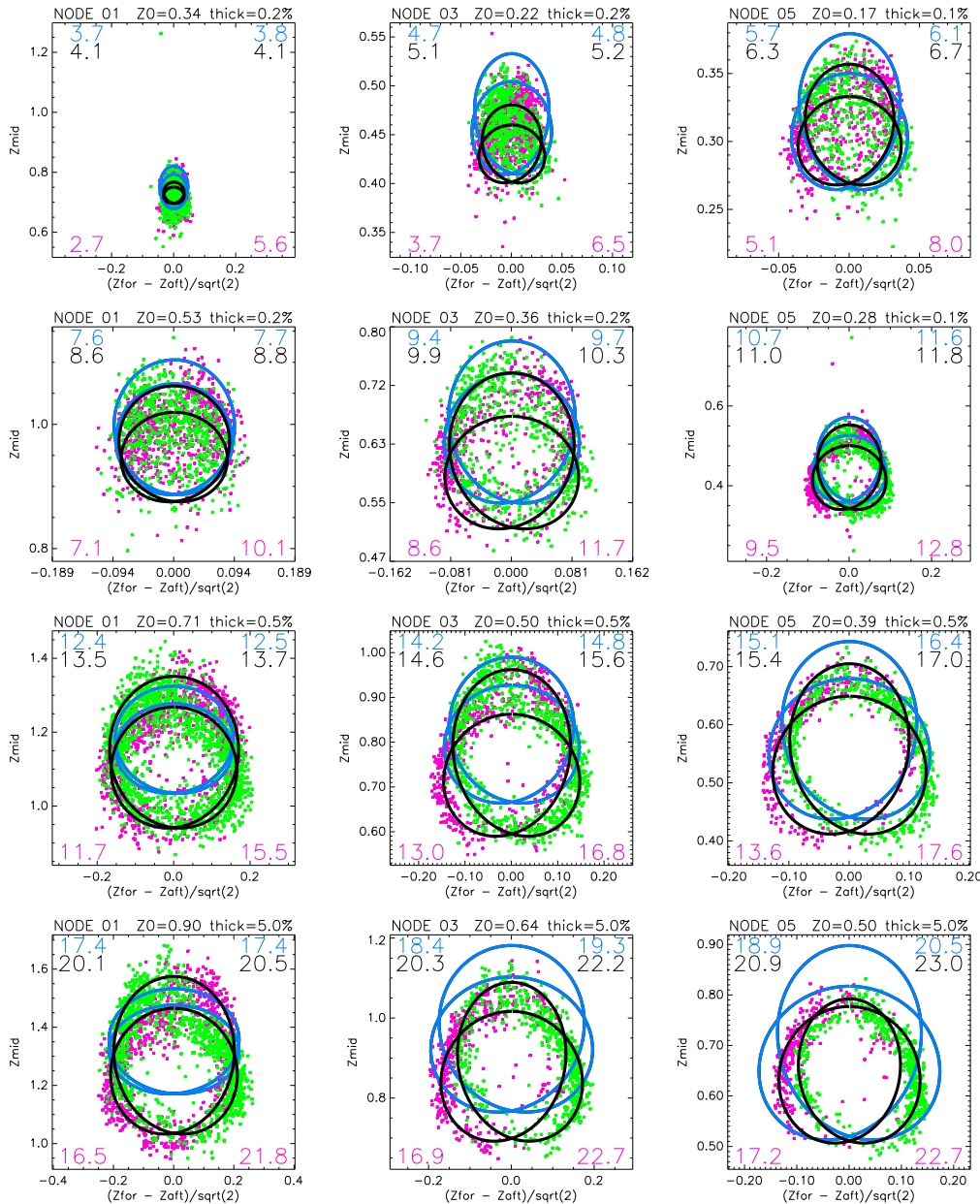


Figure 24: Cone slices for wind values of $z_0 = \sigma_0^{0.625}$ that corresponds to low to high wind speeds, for nodes 1, 3 and 5. Blue curves are cuts of the CMOD4 cone, black curves for CMOD5. Purple points are observed triplets for which the relative wind direction w.r.t. the mid-beam azimuth angle of collocated FGAT winds was between 0 and 180 degrees, green points for directions between 180 and 360 degrees. Numbers within the panels indicate average wind speed plus and minus one standard deviation (left, right respectively) for CMOD4 (blue), CMOD5 (black) and collocated FGAT winds (purple).

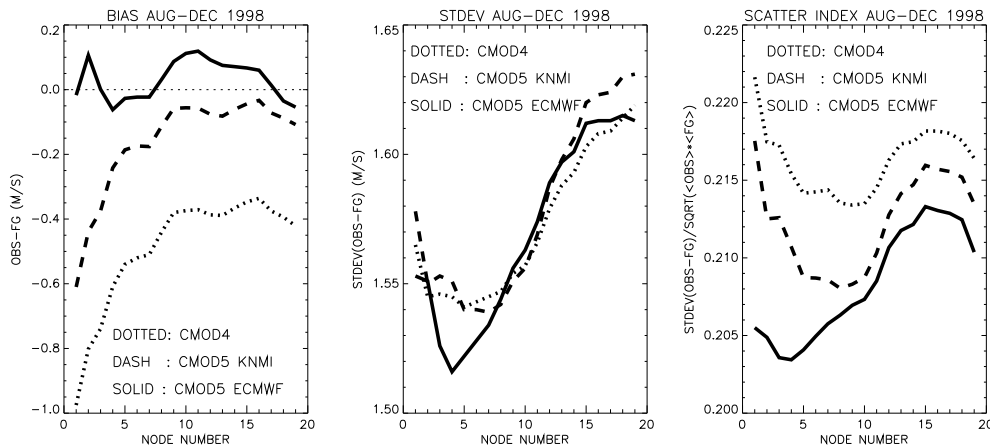


Figure 25: Wind-speed averaged bias, standard deviation and scatter index of inverted winds w.r.t FGAT winds, as a function of node number. Dotted curves are for CMOD4, dashed for CMOD5(KNMI) and solid for CMOD5.

The mathematical expressions for the three Fourier terms were constructed in an iterative way. Starting from tabulated values determined from the at KNMI developed prototype of CMOD5 (de Haan and Stoffelen, 2001), each of the three terms B_0 to B_2 was updated separately, using its own methods. This included the non-trivial task of transforming tabulated values into an appropriate functional form. In case a method required the inversion of winds, i.e., the full knowledge of the model function, the current estimate for the other two terms was used. This procedure was repeated several times, which after convergency culminated in the final definition of CMOD5, involving 28 coefficients (see the appendix in Hersbach 2003).

4.2.3 Performance and validation

In backscatter space, the CMOD5 cone corresponds in general much better to the cloud of observed triplets, than the corresponding cones defined by CMOD4 and CMOD5(KNMI) do. The model cone is to a large extent determined by the B_1 and B_2 terms. Especially for strong winds, the correct reduction of the model cone diameter, is the result of a proper redefinition of the B_2 term. In addition, for several cuts of the cone, a double loop structure observed in the data, is correctly described by the CMOD5 formulation. It is the result of a proper redefinition of the B_1 term. For low incidence angles at high backscatter values (i.e., strong winds) a shift in the mid-beam direction of the CMOD4 and CMOD5(KNMI) cone w.r.t. to the data cone has been corrected. It is the result of an improved description of the variation of the B_0 term as function of (low) incidence angle. Some examples are shown in Figure 24. The distance to the cone, which is a measure to what degree the model cone is able to describe the data cloud, is in general lowest for CMOD5. Especially, towards strong winds the CMOD5 distance to the cone decreases while it rapidly increases for CMOD4 and CMOD5(KNMI).

Only for high incidence angles at low wind speeds CMOD5 appears not to be optimal. For this combination of incidence angle and wind speed, the distance to the cone is largest for CMOD5. A reason for this non-optimal behavior is the existence of an asymmetry between the mid beam when compared to the fore and aft beam at similar incidence angle. It is induced by an underflow problem of the on-board analog to digital converter. As a result, mid-beam measurements for light winds are higher than they should be. The problem mainly occurs in the region for which backscatter values are low, i.e., at high incidence angles. The magnitude of this underflow had not been realized before.

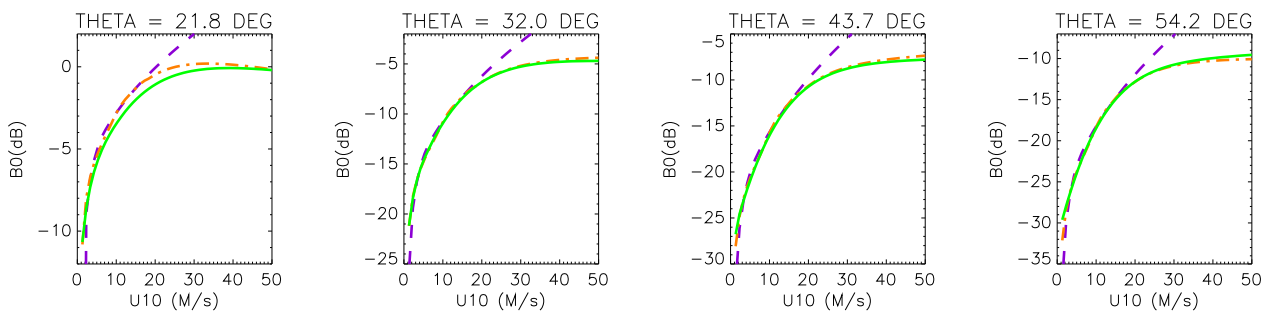


Figure 26: Formulations of the B_0 term for CMOD4 (dashed purple), CMOD5(KNMI) (dash-dotted beige) and CMOD5 (solid green).

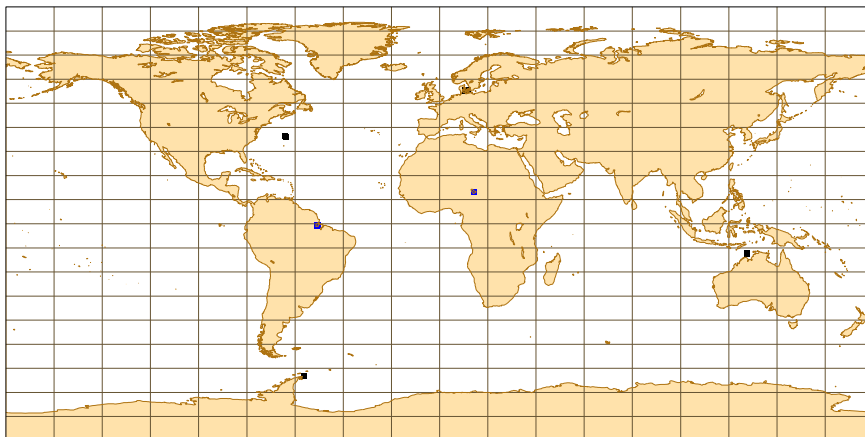
In wind space, inverted CMOD5 winds are nearly unbiased when compared to the FGAT winds for the optimization period (see Figure 25). This is true for all nodes and nearly all wind speeds. Therefore, the large negative biases of CMOD4 and the large node-dependency of the bias levels of CMOD4 and CMOD5(KNMI) have been removed. Standard deviations of CMOD5 winds relative to the FGAT winds are comparable or better than those for CMOD4 and CMOD5(KNMI). The scatter index is best for CMOD5 for all incidence angles.

The recent experimental work of Donnelly *et al.* 1999, Carswell *et al.* 1999 allowed for a realistic derivation of a model function at strong wind speeds. The over-saturation of B_0 for strong winds at low incidence angles can be seen from Figure 26. As a result, both CMOD5(KNMI) and CMOD5 give a better representation for extreme situations. In Figure 27 all inverted winds of 24 m s^{-1} or larger during the period 1 September to 31 December 1998, are plotted for CMOD4 (top panel) and CMOD5 (lower panel). As can be seen, the difference is striking. Besides the erroneous winds for the Amazon estuary, Lake Tsjaad, Antarctica and Denmark, such high winds were only observed for hurricane Danielle and tropical cyclone Thelma. For CMOD5, on the other hand, for many tropical cyclones and extra-tropical storms, retrieved winds are 24 m s^{-1} or higher. For CMOD5(KNMI) even stronger winds are observed (Hersbach 2003), especially at higher nodes. The directional flow-structure of the CMOD5 winds looks for tropical cyclones more continuous than it does for CMOD4 and CMOD5(KNMI) (see Hersbach 2003). It is likely to be the result of an improvement of the B_1 term.

The performance of CMOD5 was also tested for the periods of the month December of the years 1997, 1998 (which is part of the optimization period), 1999 and 2000. Trends in the bias levels of the CMOD winds compared to such FGAT winds were shown to arise from trends in the FGAT winds (see Appendix C). The question thus emerges, whether the FGAT winds during the optimization period were unbiased w.r.t. to 'true' winds or not. Such an answer could only be achieved by a comparison with an independent, unbiased data set (height-corrected buoy measurements are a candidate). Such a collocation study was beyond the scope of this work.

CMOD4 STRONG WINDS 19980801-19981231

■ 24 - 26 ■ 26 - 28 ■ 28 - 30 ■ 30 - 32 ■ 34 - 50



CMOD5 STRONG WINDS 19980801-19981231

■ 24 - 26 ■ 26 - 28 ■ 28 - 30 ■ 30 - 32 ■ 34 - 50

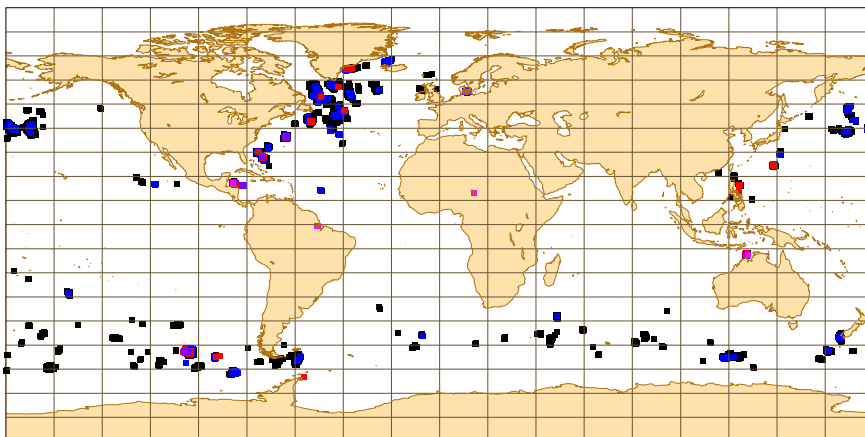


Figure 27: Retrieved ERS-2 winds of 24 m s^{-1} and higher in the period August-December 1998. The top panel shows results for CMOD4 inversion, the lower panel for CMOD5.

5 Conclusions and Recommendations

Continuous monitoring and verification of the ERS-2 fast delivery wind and wave products from RA (URA), SAR (UWA) and scatterometer (UWI) are carried out routinely at ECMWF. Data from ECMWF atmospheric (IFS) and wave (WAM) models and from in-situ buoy observations are used for this purpose. ERS-2 suffered from the loss of some of its gyros since early 2000. The platform was piloted using a single gyro since then. ERS-2 situation became worse due to the loss of more gyros early 2001. This led to the zero gyro mode piloting since June 2001. As a result, several products were degraded. The main victim was the UWI product, which became of poor quality forcing ESA to halt its dissemination. ESA managed to improve the quality of the UWI product. The quality of the UWI product has been closely monitored at ECMWF since 12 December 2001. The degradation impact of zero-gyro mode was less pronounced on the URA and UWA products. Examining the results of the monitoring and validation of ERS-2 wind and wave products leads to the following conclusions with appropriate recommendations:

- The radar altimeter significant wave height product is generally of good quality (apart from the over-estimate of the lower wave heights). It sustains a rather stable performance. The agreement between altimeter and WAM wave heights is improving in time.
- RA wave height histograms agree rather well with the model counterparts. However, a secondary peak at wave height around 2.5 m is of some concern. Such peak does not exist in the corresponding off-line product, model or ENVISAT (both Ku and S band) histograms. The reason behind this secondary peak is not clear. Examining this feature is one of our recommendations.
- The activation of the ZGM on the platform AOCS (June 2001) led to slight degradation in the altimeter wave height product.
- The implementation of the new yaw control system (March 2002) seems to have a positive impact on the altimeter wave height product. A model change around that time might have some contribution towards this result.
- The relative random error of RA significant wave heights was estimated using multiple collocation techniques to be around 7% for super-observations and around 10% for individual observations. Furthermore, the altimeter waves are lower than the buoy waves by about 3%.
- RA wind speed products are less stable with several periods of poor performance especially after the loss of the platform gyros. Sun blinding effect between January and March each year since 2000 is responsible for most occasions of poor performance. The ZGM in early June 2001 was also responsible before the implementation of the new yaw control system in March 2002.
- Apart from the sun blinding effect, RA wind product seems to be stable and of good after the implementation of the yaw control system.
- The altimeter backscatter statistics witnessed significant change by the beginning of year 2000, when ERS-2 started to lose its gyros. Peaks of monthly mean backscatter values used to occur in July each year missed since 2000. Sharp drops in the mean values started to occur in February each year since 2000 due to the sun blinding effect.
- The altimeter backscatter histogram witnessed significant change as well. The monthly histogram of backscatter is used to have a well-defined single peak. Starting from early 2000, an important secondary peak started to emerge and sometimes it becomes as important as the primary peak. Lately, we started to have double-peaked histograms.



- It is recommended that an investigation be made to explain the change of the statistics and the distribution of the backscatter. Such investigation may be crucial if the ERS-2 RA backscatter is used to calibrate ENVISAT RA-2 backscatter.
- SAR wave product is rather stable except for the year 2001. There was a bug in the inversion software at ECMWF between June 1998 and November 2000. This bug caused relatively high bias and RMSE. The fix to this bug led to good agreement with the wave model results.
- The loss of the platform gyros in January 2001 worsens the SAR performance. Apparently, the ZGM led to slight improvement. The significant improvement happened in December 2001. The reason for this improvement is unknown. The new yaw control system of March 2002 does not seem to have much impact on the SAR wave heights.
- The large errors in the yaw attitude control that emerged after the loss of ERS's gyroscopes in January 2001, had a decremental effect on the quality of the UWI product. This forced ESA to suspend its world-wide dissemination. On 12 December 2001 ESRIN restarted distribution of UWI data, however, to a selective group only. Monitoring at ECMWF showed that the product was initially poor. However, steady improvement towards the level obtained during the nominal period (i.e., before January 2001) was observed.
- The introduction of ESACA on 4 February 2003 was a large step forwards in the quality of the UWI product. The analysis performed at ECMWF showed that the potential quality of this data is high. Since this introduction, the standard deviation of winds inverted on the basis of CMOD4 and CMOD5 versus FGAT winds is lower than it was during the nominal period. However, several shortcomings were detected. Feedback with ESRIN helped ESRIN to identify the problems and find the appropriate solutions. An example is the detection of the disagreement between UWI winds and CMOD4 winds.
- The work on CMOD5 was completed. Starting point was a prototype of CMOD5 developed at KNMI. CMOD5 does not show the undesired saturation for strong winds as it is observed by CMOD4, and inter-node differences have largely been removed.
- The derivation of CMOD5 revealed an underflow problem of the mid beam. Triggered by these findings, the ERS-2 antenna gain was increased by 3 dB on 28 February 2003.
- At the 22nd ASCAT Science Advisory Group Meeting at ESTEC (18-19 September 2002), CMOD5 was adopted as the new state-of-the-art wind model for C-band scatterometry. In addition, the group recommended that CMOD5 should be the baseline for the generation of ASCAT winds. This instrument, which is part of the payload of the METOP missions, is expected to be launched mid 2005.
- After the completion of its test phase (July 2003), ESRIN plans to restart worldwide dissemination of ERS-2 scatterometer data. At ECMWF assimilation experiments including UWI data in ZGM using wind inversion on the basis of CMOD5 are being performed. Aim is to introduce its operational assimilation as soon as possible.

Acknowledgments

The work presented in this paper was funded by ESRIN (Project Ref. 15988/02/I-LG). We would like to thank Peter Janssen, Jean Bidlot and Lars Isaksen, for support and valuable discussions.

A Appendix: Processing of ERS-1/2 URA Data

A.1 Introduction

The wind and wave data collected by the Radar Altimeter (RA) on-board ERS-1 and ERS-2 satellites are received in BUFR format at ECMWF through the Global Telecommunication System (GTS). This product, which is also called the "User Fast Delivery RA (URA) Product", is monitored daily by ECMWF. The product passes through the quality control procedure described below. The data then are collocated with and verified against ECMWF wave model (WAM) first-guess data on a daily, weekly and monthly basis. Furthermore, the data are collocated with and verified against the in-situ wave buoys and platform wind and wave measurements on a monthly basis. Monthly reports describing the results of this performance monitoring and geophysical validation are prepared and sent to ESA-ESRIN.

The URA significant wave height values that pass the quality control are assimilated into the operational ECMWF wave model. This assimilation is important to improve the "nowcast" of the model and to provide more accurate initial condition for the medium-range wave forecast (up to 10 days). The URA wind speed data are not assimilated into the ECMWF atmospheric model. Therefore, the wind speed information is used as a diagnostic tool for the model output.

A.2 Quality Control procedure

The URA product is collected for time windows of 6 hours centred at major synoptic times ending at 12:00 UTC going back (i.e. 18 UTC of previous day and 00, 06 and 12 UTC on that specific day). This configuration is used to go in parallel with the ECMWF operational system. The data are stored in a file with the internal naming convention of "URAYyyyymmddhhnn", where yyyy is the year, mm is the month, dd is the day, hh is the hour and nn is the minute of the centre of the time window. This file is nothing but the URA products for the whole time window extending from time yyyymmddhhnn-3 hours to yyyymmddhhnn+3 hours in BUFR format. The quality control process can be divided into two

1. A basic level: to ensure that each individual observation is within the logical range and is collected over water, during the correct time window.
2. A secondary level: to ensure that observations within any given sequence are consistent with each other. Observations passing the first level enter into this level. It is important to mention that this classification is just for clarification purposes and has no consequence on the quality control process itself.

A.2.1 *Basic Quality Control*

The URA product is first decoded. Any record with missing value of any key parameter (time, location, backscatter, significant wave height, wind speed,.. etc.) is considered as a corrupt record and is not included at any stage of quality control process (as if it does not exist). The records belong to the current time window but found in the files of the previous windows (see below), are read in (if any). All the observation records are then sorted according to the acquisition time. The records are checked to detect any duplicated observation. One of those duplicates is retained while the other(s) is/are rejected by setting the "double-observation flag" (quality flag number 6) to 1.

If the peakiness factor, which is a measure of the degree of peakiness in the return echo and is supplied as part of the URA product, is very high, the record should be rejected as this is an indication of the existence of sea



ice contaminating the observation. The threshold value for the peakiness factor selected is 200 based on some empirical numerical tests by Bidlot and Hansen (2000). The peakiness factor in this context is defined as:

$$\text{Peakiness Factor} = 100P(t)_{\max}/[2 \langle P(t) \rangle] \quad (1)$$

where $P(t)$ is the echo power as a function of time t , $P(t)_{\max}$ and $\langle P(t) \rangle$ denote the maximum and mean values of the echo power. Therefore, if the peakiness factor exceeds the threshold value (=200), the record is rejected by setting the "peakiness flag" (quality flag number 7) to 1.

If the observation is found to belong to any of the previous time windows, it is assumed that it is too late to process this observation and the record is rejected by setting the "model-domain flag" (quality flag number 1) to 1 to indicate an "outside time-window" condition. If the observation belongs to a later time window, the record is removed from the observation set and written into a file that will be read at next time window.

The observation is then collocated with the operational WAM model by locating the RA observation on the land-sea mask of the model. The currently used land-sea mask is an irregular (reduced) latitude-longitude grid with resolution of 0.5° (around 55 km in both directions). If the observation is collocated with a land point, the record is rejected by setting the "model-domain flag" (quality flag number 1) to 2 to indicate a "land-point" condition. If the observation is collocated with a grid point outside the grid area (e.g. over ice), the record is rejected by setting the "model-domain flag" (quality flag number 1) to 3 to indicate an "outside grid area" condition.

The value of the RA significant wave height (SWH) is checked to make sure it is within the accepted logical range. If the wave height is found to be below the accepted minimum (0.10 m is used) or above the accepted maximum (20.0 m is used), then the record is rejected by setting the "SWH logical-range flag" (quality flag number 2) to 1.

A.2.2 Consistency Quality Control

The observations that pass the basic quality control go through the second level of quality control, which includes several consistency tests. The RA observations are grouped as sequences of neighboring observations. The maximum number of individual observations within each sequence is selected as 30 observations. This selection was made in the early days of the ERS missions when the resolution of the ECMWF WAM model was 3 degrees (more than 300 km) and later reduced to 1.5 degrees (more than 150 km). The value of 30 was never changed.

The sequence construction starts by selecting the first record passes the basic quality control in the time window under consideration as a possible candidate to be the first member in the sequence. The time and the SWH observation of the next record is compared with those of the already selected record. If the time difference between both records is more than an allowed maximum duration (3 s is used) or if the absolute difference between both SWH's exceeds an allowed maximum value (2.0 m is used), then it is assumed that there is a jump over a gap (i.e. an island, a peninsula, ... etc.). The previous record is removed from the sequence and is rejected by setting the "gap-jump flag" (quality flag number 3) to 1. The current record then becomes the first record in the sequence. Then the same procedure is repeated until we have two records accumulated in the sequence.

More records are recruited to the sequence in the same manner until either a gap is detected (using the time difference or the SWH difference) or until the maximum number of observations in the sequence is reached. If a gap is detected and the number of the records accumulated in the sequence is less than a predefined minimum

(20 records is used), all of the already selected records are rejected by setting the "observation-sequence flag" (quality flag number 4) to 1 to indicate a "short sequence" condition. If the number of observations in the sequence exceeds the predefined minimum (including if the maximum number has been reached), then the sequence goes through further quality control tests. Then the mean and the standard deviation of the observations accumulated in the sequence are computed.

The next step is to eliminate spikes by rejecting observations with SWH outside the 95% confidence interval. To accomplish this, we compute the SWH confidence limits of the sequence as:

$$\text{Confidence Interval} = \min\{\alpha, \zeta \cdot \sigma\} \quad (2)$$

where α is a maximum value of the confidence interval (used as 2.0 m in the first iteration and as 1.0 m in the second iteration), ζ is a factor for the spike test (a value of 3 is used), and σ is the standard deviation of SWH. If the absolute value of the difference between the SWH of the individual record and the mean SWH of the sequence exceeds the confidence interval computed by Eq.(2), then that individual record is rejected by setting the "confidence-interval flag" (quality flag number 5) to 1. The flagged records are removed from the sequence and another spikes-removal iteration is carried out using the modified sequence and a rather stricter confidence interval condition (in Eq.(2), the value of 1.0 m for α is used in the second iteration).

If the number of individual records passed the spikes test in the sequence is less than the minimum allowed (20 records), all the records are rejected by setting the "observation-sequence flag" (quality flag number 4) to 1 to indicate a "short sequence" condition. If there are enough records, the mean and standard deviation of SWH, backscatter and wind speed, the mean geographical coordinates and the mean time of the sequence with the records passed the spikes test are computed. This is called the "super-observation". Finally, the variance of the SWH values in the sequence is tested. The maximum allowed SWH variability within the sequence is given by:

$$\text{Maximum SD} = \max\{\beta, \gamma \cdot \mu\} \quad (3)$$

where β is the minimum allowed standard deviation (0.5 m is used), γ is a factor for the variance test (0.5 is used) and μ is mean value of SWH in the sequence. If the standard deviation of the SWH exceeds the maximum value computed by (3), all records in the sequence are rejected by setting the "observation-sequence flag" (quality flag number 4) to 2 to indicate a "noisy observation-sequence" condition.

The same procedure is repeated by selecting a new sequence until all the observations within the current time window are processed.

A.2.3 Output Files

The quality control procedure described above generates two types of files: "Radar flagged" (RFL) file, and "Radar averaged" (RAV) file. Furthermore, it appends a record in an "extended statistics file" (ESF) for each time window representing the statistics of quality control procedure for that specific window. The ESF file is used to plot the time series of data received, data rejections and data acceptance.

All records processed are written together with their corresponding flags in the "Radar flagged" file with the following naming convention: "RFLyyyymmddhhnn". This file contains the complete information included in the URA product with the values of the 7 quality flags listed in Table 1 and described in Sections A.2.1 and A.2.2. This file covers the time period extending from time yyyymmddhhnn-3 hours to yyyymmddhhnn+3 hours in FORTRAN binary format. This file is converted to BUFR using the "enderac" utility program. The

Flag No.	Quality Flag Name	Value	Meaning
1	Model-Domain	1	Observation is outside the time window (belongs to previous time window).
		2	Observation is over land.
		3	Observation is outside the WAM grid area (possibly over ice)
2	SWH Logical-Range	1	SWH observation is out of range (either less than 0.1 m or more than 20 m)
3	Gap-Jump	1	Jump before or behind a gap (e.g. island).
4	Observation-Sequence	1	Short sequence (too few of accepted observations in the sequence).
		2	Noisy SWH observations in a sequence.
5	Confidence-Interval	1	Observation is outside the 95% confidence interval
6	Double-Observation	1	This is a replicate observation.
7	Peakiness	1	The peakiness factor is too high (possibly water is ice contaminated).

Table 1: The Quality Flags used in the Quality Control Procedure (the observation record passes quality control if all 7 quality flags are zeros).

name convention of the BUFR version is: "BFLyymmddhhnn". This file is an important product that can be used instead of the original URA product. For example, this file is used as the input to the data assimilation procedure where only observations passed the quality control are used in assimilation.

The super-observations (i.e. the means and standard deviations of the sequences with records passed the quality control) are written to the "Radar averaged" file with the following naming convention: "RAVyyymmddhhnn". This file contains the sequence means and standard deviations for the whole time window extending from time yyyymmddhhnn-3 hours to yyyymmddhhnn+3 hours in FORTRAN binary format. This file is converted to BUFR using the "enderac" utility program. The name convention of the BUFR version is: "BAVyyymmddhhnn". This file is not of much practical interest as it is considered as an intermediate medium to pass the averages needed in the next step which is the RA-WAM collocation.

A.2.4 RA Model Collocation

After the quality control and averaging process, the individual RA SWH observations that pass the quality control are prepared for the data assimilation. To be specific, the RFL file is used for this procedure. The individual observations within the catchment area of a grid point (i.e. within a box with dimensions of grid increment and centred on the grid point) are averaged and assigned as the SWH observation corresponding to that grid point. The model is run to produce the first-guess fields. The data assimilation procedure is then used to blend the first guess fields with the RA observations to produce the analyzed fields.

The ECMWF analysis wind velocity fields and the various WAM first-guess wave (SWH, mean wave direction, mean wave period, peak wave period,.. etc.) fields are interpolated over a regular grid of 1.5° by 1.5° at all analysis times (00:00, 06:00, 12:00, and 18:00 UTC). Each RA super-observation represented by the mean time and position of the corresponding sequence in the RAV file is collocated with the nearest model grid point. The values of the model parameters at the corresponding grid point and at the previous and next analysis times are interpolated at the mean time of the super-observation. The super-observation record and the time-interpolated model parameters are all written in the RA-WAM collocation (RAC) file. The name convention of this file is: "RACyymmddhhnn" covering the time period extending from time yyyymmddhhnn-3 hours to

yyyymmddhhnn+3 hours. The file is written in FORTRAN binary format. This file is converted to BUFR using the "enderac" utility program. The name convention of the BUFR version is: "BACyyyymmddhhnn".

A.2.5 RA Buoy Collocation

In-situ wind and wave observations, which are collected by ships, buoys and platforms (for simplicity, all will be called hereafter: "buoy data"), are routinely received at ECMWF through the GTS and archived. Significant portion of the buoy data arrives with some delay. In general, most of the buoy data arrives within 48 hours of the acquisition time.

Most of the buoy observations are collected on hourly basis. The remaining part may be collected at lower frequencies (e.g. 3 hours). The buoy observations collected 2 hours earlier and later than an analysis time (5 observations) are averaged and assigned to be the buoy observation at that analysis time. This buoy observation is collocated with the nearest model grid. The averaged buoy observations and the model analysis parameters (namely: SWH, mean wave direction, peak wave period, wind speed and direction, MSL pressure, air and seawater temperatures) are written to a collocation buoy-model (CBM) file. This task is run operationally every day with a lag of two days to ensure the arrival of most of the buoy data.

The triple-collocation (RA-model-buoy collocation) exercise is done at the beginning of each month (on the 4th of the month) for the whole of the previous month. The contents of the RAC (see Section 3) and the CBM files are used. A RAC record is collocated with a CBM record if the following two conditions are satisfied:

1. both the RA super-observation and the buoy observation are assigned to the same analysis cycle; and
2. the distance between the RA super-observation and the buoy is within a given distance (200 km is used).

Each collocated pair of records are merged as one record and written to a collocation altimeter-buoy (CAB) file. The name convention of this file is: "CAByyyymm010000" covering the whole month of mm of year yyyy. The file is written in FORTRAN binary format. This file is converted to BUFR using the "enderac" utility program. The name convention of the BUFR version is: "BACyyyymm010000".

B Appendix: Processing of ERS UWA Data

The SAR data received at ECMWF is gathered in batches covering 6-hour time windows centred at major synoptic times (00, 06, 12 and 18 UTC). The data contents of each batch is preprocessed to generate a list with output positions for the WAM model in order to produce a collocation file of wave spectra to be used for the SAR-inversion system. This procedure includes basic pre-processing quality control checks to reject any data with obvious anomalies and/or inconsistencies. The product parameters are checked and if any is found to be not logical, a quality control indicator (JFL300) is set as follows:

1. incorrect satellite flight direction
2. incorrect satellite incidence angle
3. incorrect satellite altitude
4. incorrect satellite velocity
5. incorrect number of azimuthal looks

6. incorrect azimuthal resolution
7. incorrect radar frequency
8. incorrect radar polarization
9. incorrect radar look direction

If any of the above conditions occurs, the observed SAR spectrum is rejected and not processed. In the statistics, the rejected observations due to the above reasons are accounted to IREJQF.

The nearest WAM grid point coordinates are recorded in order to be used later to extract the WAM wave spectra which will be used as the first guess to invert the raw UWA product. The observed SAR spectra are then inverted to calculate the corresponding wave spectra by an iterative method based on the forward closed integral transformation (what is termed as the MPI scheme). The first guess to start the iteration is extracted from the WAM model run. The first-guess wave spectrum is used to simulate an initial "iterated" SAR spectrum using the full nonlinear mapping relation.

The first-guess wave spectrum and the observed spectrum are further examined for possible problems. So before the start of the inversion procedure, the quality control indicator (JFL300), that was mentioned above, is set as follows:

10. the observed SAR spectrum is rejected as it was not possible to collocate it with an appropriate first-guess wave spectrum (the observation is either outside the time window or was done over ice). For the statistics purposes, such rejections are accounted to IREJEC.
11. the first-guess wave model represents very low wave conditions ($H_s < 0.1$ m). For the statistics purposes, such rejections are accounted to IREJHZ.
12. very noisy observed SAR spectrum ($s/n < 3$ dB). Such rejections are accounted to IREJUW.
13. currently not used!
14. very noisy simulated SAR spectrum ($s/n < 3$ dB) before starting the iterations. Such rejections are accounted to IREJSZ.

If any of the above conditions occurs, the observed SAR spectrum is rejected and not processed. The JQUAL flag (see below) is set to 4.

The "retrieved" (best fit) wave spectrum is found by minimizing a cost function that penalizes three differences which are:

1. the difference between the observed and "iterated" SAR spectra,
2. the difference between the first-guess and "iterated" wave spectra, and
3. the difference in the azimuthal cut-off wave number of the observed and "iterated" SAR spectra.

Finally, a new first-guess wave spectrum is constructed using the best guess "iterated" wave spectrum and another round of iteration using the new first guess is carried out. This would ensure the smoothness of the final "inverted" spectrum and its lowest dependence on the first-guess spectrum.

The resulting inverted spectra are flagged depending on the first-guess status, the ASAR spectrum quality and inversion results. An inversion quality indicator (JQUAL) is used to reflect one of the following conditions:

0. excellent: the inversion cost is less than 0.1
1. good: the inversion cost is in between 0.1 and 0.5
2. questionable: the inversion cost is more than 0.5
3. inversion with unstable iterations (and even for low costs it is still questionable)
4. no inversion was done as the observed SAR spectrum is rejected before starting the inversion procedure (JFL300 equals to 10 or more)
5. inverted spectrum is rejected as the best fit SAR wave spectrum (during the iterations) represents very low wave conditions ($H_s < 0.1$ m). Such rejections are accounted to IREJHS
6. inverted spectrum is rejected as the simulated SAR spectrum (during the iterations) becomes too noisy ($s/n < 3$ dB). Such rejections are accounted to IREJSN
7. inverted spectrum is rejected as it was not possible to make any azimuthal clutter cut-off adjustment.

Various statistics related to observed, first-guess and best fit SAR spectra together with the correlation coefficients between the combinations of the spectra are computed. This part of the software is responsible for the generation of the SAR-WAM collocation files.

The tasks described above are running daily with the operational ECMWF weather (and wave) forecasting system (starts around 20:00 UTC for the 24-hour period ending at 12:00 UTC).

C Appendix: Related Model Changes

Note: All changes were introduced at time-window centered at 18:00 UTC.

21 Jun. 1992 Operational implementation of the global model on a 3 degree latitude-longitude grid (63° S to 72° N). The wave spectrum is discretized using 12 directions and 25 frequencies (from 0.041772Hz).

15 Aug. 1993 Assimilation of ERS-1 RA wave heights in global model.

3 Jul. 1994 The global model horizontal resolution was increased to 1.5 degree (from 81° N to 81° S).

19 Sep. 1995 New windsea/swell separation scheme.

30 Jan. 1996 Changes to IFS (e.g. 3DVAR operational).

1 May 1996 Assimilation switch from ERS-1 to ERS-2 RA wave heights.

1 Jun. 1996 Changes to IFS to switch the assimilation of scatterometer winds from ERS-1 to ERS-2.

4 Dec. 1996 The global model horizontal resolution was changed to a 0.5 irregular latitude-longitude grid, with an effective resolution of about 55 km (from 81° N to 81° S). Change the wave-model integration scheme to accommodate Hersbach and Janssen new limiter.

13 May 1997 Modification of the advection scheme by defining the first direction as half the directional bin.

27 Aug. 1997 Changes to IFS (e.g. scatterometer winds are no longer blacklisted for speeds above 20 m/s and modification to the scatterometer bias).

11 Nov. 1997 Changes to IFS (e.g. modification of the scatterometer QC).

25 Nov. 1997 Changes to IFS to implement the 4D-Var assimilation scheme.

1 Apr. 1998 Changes to IFS model (e.g. change horizontal resolution to T319).

28 Jun. 1998 Operational implementation of the coupling between WAM and IFS.

9 Mar. 1999 10 m winds are used in coupled model. IFS changes (e.g. change vertical resolution to 50 levels, and modification of the scatterometer QC).

13 Jul. 1999 RA wave height correction based on non-gaussianity of the sea surface elevation. Change to the frequency cut-off in the integration scheme. IFS changes (new physics/dynamics coupling).

12 Oct. 1999 Changes to IFS model (e.g. change vertical resolution to 60 levels, and new orography)

11 Apr. 2000 RA data quality control based on peakiness factor. Penalization of low altimeter wave heights in data assimilation. An extra iterative loop to determine the surface stress.

27 Jun. 2000 Sea ice fraction is used for the ice mask. The buoy validation software was upgraded to use the proper anemometer height.

11 Sep. 2000 Assimilation scheme in IFS changed to 12 hour 4D-Var.

20 Nov. 2000 Increase the horizontal resolution of the atmospheric model to T511 (around 40 km). Increase spectral resolution in the global deterministic WAM model to 24 directions and 30 frequencies. Improved advection scheme on irregular grids. New empirical growth curves in the RA data assimilation. Bug fix of the SAR inversion software to properly use SAR data with the new calibration procedure (the bug was effective since June 1998).

11 Jun. 2001 IFS modifications.

21 Jan. 2002 Modified scheme for the time integration of the source terms. Assimilation of QuikSCAT data in IFS model.

8 Apr. 2002 Inclusion of wind gustiness and air density effect. Removal of spurious values for the Charnock parameter. Blacklisting procedure for wave data.

16 Apr. 2002 Extra quality control for QuikSCAT.

13 Jan. 2003 Assimilation of ERS-2 SAR data. Background check for altimeter data during assimilation. Significant changes to the IFS model.

References

- Bidlot, J. R. and B. Hansen (2000). Key features of the wave model contribution to CY22R1. *ECMWF Research Department Memorandum*, R60.9/JB/15, 13 p., ECMWF, Reading, England.
- Carswell, J. R., Castells A., Knapp E. J., Chang P. S., Black P. G. and F. Marks, (1999). Observed Saturation in in C and Ku-band Ocean Backscatter at Hurricane Force Winds. *unpublished*.
- Donnelly, W. J., Carswell J. R., McIntosh R. E., Chang P. S., Wilkerson J., Marks F., and P. G. Black (1999). Revised Ocean Backscatter Models at C and Ku-band under High-wind Conditions, *J. Geophys. Res.*, **104** (C5) 11,485-11,497.
- Haan, de, S and A. C. M. Stoffelen, (2001). CMOD5, **SAF/OSI/KNMI/TEC/TN/140**, www.eumetsat.de/en/area4/saf/internet/other_reports/SAFOSI_W_cmod5-knmi.pdf, EUMETSAT-Publications Division, EUMETSAT, Darmstadt, Germany.
- Hersbach, H., (2003). CMOD5. An improved geophysical model function. *ECMWF Technical memorandum 395*, ECMWF, Reading, England.
- Isaksen, L., and P. A. E. M. Janssen (2003). The benefit of ERS Scatterometer Winds in ECMWF's variational assimilation system. To be submitted to Q. J. R. Meteorol. Soc.
- Janssen, P. A. E. M. and S. Abdalla (2003). Verification of ENVISAT RA-2 wind and wave products, *poster EAE03-A-02558; G13-IWE3P-0667*, presented at the EGS-AGU-EUG Joint Assembly, Nice, France, 06-11 April 2003. Abstract in Geophysical Research Abstracts, Vol. 5, 02558, 2003 published by the European Geophysical Society.
- Janssen, P. A. E. M., B. Hansen, and J. R. Bidlot, (1997) Verification of the ECMWF wave forecasting system against buoy and altimeter data, *Wea. Forecasting*, **12**, 763-784.
- Janssen, P. A. E. M., S. Abdalla, and H. Hersbach (2003) Error estimation of buoy, satellite and model wave height data model wave height data. *ECMWF Technical memorandum 402*, ECMWF, Reading, England.
- Stoffelen, A. C. M., (1998). Error modeling and calibration; towards the true surface wind speed, *J. Geophys. Res.*, **103**, (C4) 7,755-7,766.